

# THE USE OF VORONOI BINNING IN OBTAINING COLOUR PROFILES OF FDS DWARFS

Determining Fornax dwarf galaxy colours down to low surface brightness levels using FDS data and Voronoi binning.

## Abstract

With the use of Voronoi-binning and masks it is investigated up to which extend from the source's centre, the colour of various dwarf galaxies captured in the FDS can be determined. In addition, various RGB images are created.

Marloes J.L. Bodegom, S3339831  
31-03-2021 Supervised by R.F. Peletier

## Project Aim

The aims of this project can be divided into roughly three goals, two of which are research goals. The last goal relates to the broader context of the project.

1. The main question examined in this project is whether applying Voronoi binning will enable one to determine the colour profile of dwarf galaxies within a certain accuracy up to lower levels of surface brightness compared to not binning the data.
2. The second objective of this project is to create RGB pictures of dwarf galaxies from FDS data which look realistic and preserve their characteristics regarding colour and structure.
3. From the perspective of the study of science communication, the aim of the project is to gain insight into the process of conducting research.

## Contents

Project Aim .....	1
Introduction.....	4
Theory.....	5
Chapter 1: The Fornax Deep Survey.....	5
Fornax Cluster.....	5
FDS.....	5
NGC1427A .....	6
VST and OmegaCAM.....	7
Chapter 2: Removing the background.....	8
Dataset .....	8
NGC1427A .....	8
Removing the background .....	10
Grid oriented .....	10
Histogram approach.....	10
Systematic noise estimate.....	11
FDS-Band specific noise.....	12
Masks.....	12
Chapter 3: Voronoi Binning.....	14
Voronoi diagram.....	15
Voronoi Binning.....	15
WVT .....	17
Chapter 4: colour profiles and RGB images.....	19
Colour .....	19
Colour computation .....	19
RGB image creation.....	19
Methods .....	21
Chapter 5: Computations .....	21
The process.....	21
Step 1: Acquiring the data .....	21
Step 2: Background reduction .....	21
Step 3: Voronoi binning.....	22
Step 4: Making the profile .....	22
Step 5: The error.....	24

Results .....	25
Chapter 6: RGB image results.....	25
Filenames .....	25
Series 6: colour differences per filter (autod#/ds9_ugr_realistic.png) .....	25
Chapter 7: Research Results.....	27
FDS10_DWARF023 .....	27
FDS10_DWARF189 .....	30
FDS10_DWARF034 .....	33
FDS10_DWARF359 .....	35
Discussion.....	38
Background reduction .....	38
RGB creation.....	38
Colour profiles .....	39
General Remarks .....	39
Conclusion .....	40
Acknowledgements .....	42
References.....	43
Appendix A: an overview of Voronoi binned g-r diagrams with varying target signal to noise.....	45
Appendix B: Tile 11 dwarf galaxy RGB-images of the g- (blue), r- (green) and i- (red) bands. ....	49
Appendix C: Tables/factsheets .....	54
FDS10_DWARF023 .....	54
FDS10_DWARF034 .....	55
FDS10_DWARF189 .....	56
FDS10_DWARF359 .....	57
Appendix D: Image series 0-5.....	58
Series 0: Astropy's make_lupton_rgb() (d#_ugr.png) .....	58
Series 1: ASINH DS9 (ds9_d#_ugr.png) .....	58
Series 2: LOG DS9 (ds9_d#_ugr_log.png).....	59
Automation.....	59
Series 3: logarithmic images (autod#/ds9_ugr.png) .....	59
Series 4: bright logarithmic images (autod#/ds9_ugr_bright.png).....	60
Series 5: bright linear images (autod#/ds9_ugr_bright_lin.png) .....	60
Appendix E: scripts .....	61

## Introduction

Colours, like g-r, play an important role when determining the stellar population of galaxies. By examining colour gradients, one can determine variations in the population. One can, for example, examine whether the population at the outskirts of a galaxy is younger than stars near its centre. Colour gradients are of great scientific importance as they indicate how the age and metallicity of a galaxy vary as a function of its radius. This can provide information on processes which regulate the growth and assembly of galaxies, such as whether there has been late infall, as well as internal processes, like stellar migration (Parikh et al. (2021)).

Preferably one would like to make colour profiles that reach as far from the centre as possible. Unfortunately it is, however, often difficult to accurately determine the colour of a galaxy far away from its centre, due to various problems that may be encountered, which will be discussed in this report.

For any galaxy, if one goes far away enough from the centre the sky background will dominate and hide the galaxy's signal. The image of sky is often not flat and thus cannot be subtracted easily. In addition there may be stars on the foreground or reflections caused by e.g. the telescope's setup. At low surface brightness the impact of these features, the noise, becomes large, making it very difficult to go deep. In this report we try to overcome this problem of a low signal to noise ratio by applying Voronoi binning and by testing whether masking the signal from external sources near the observed source helps to further improve the results.

The data used to create the colour profiles comes from the FDS, Fornax Deep Survey. Several dwarf galaxies of varying masses and brightness are examined and their g-r colour profiles are computed without binning and using Voronoi binning. Voronoi binning is an adaptive binning method that results in an increasing bin size with decreasing signal.

The main aim of this research is to use Voronoi binning to accurately determine the colour, the relation between the intensity in two different bands, of a dwarf galaxy at larger distances from its centre. To verify whether this is the case, Voronoi binned colour profiles of FDS dwarfs will be compared to their non-Voronoi binned equivalents. In addition it is tested whether masking the signal from external sources near the observed source helps to further improve the results.

To make reliable colour profiles of the dwarfs, it is of importance to first get acquainted with the data and programs used. In the first stages of the research, most time was spent on this aspect whilst working on the second goal of this project: to develop appealing RGB images of the dwarf galaxies from the FDS data. This led to several series of images with increasing quality as described in chapter 6.

This report begins by providing background information on the Fornax cluster and the FDS, along with the underlying theory for the conducted research. Next, the scripts developed for the data processing as well as the restrictions set and assumptions made along the data journey are described in detail, after which the results are presented. Lastly the results and the research process are critically examined and the final conclusions are presented as well as several recommendations for future research.

## Theory

### Chapter 1: The Fornax Deep Survey

#### Fornax Cluster

The Fornax cluster, which is shown in figure 1.1, is a dense cluster of galaxies approximately 20 million parsec away from Earth. Its name originates from its location in the constellation of Fornax, which is derived from the Latin word for oven. The cluster is centred around NGC1399. The Fornax cluster contains many dwarf galaxies: 564 dwarf galaxies located in the cluster have been catalogued in the *Fornax Deep Survey with VST. IV. Dwarf galaxies* (Venhola et al., 2018) catalogue (FSDC)<sup>1</sup>. The dwarf galaxies vary in properties, consider for example the bright and irregular NGC1427A and the faint and elliptical FDS11\_DWARF071b. The cluster is located at circa 3h 38m Right Ascension (R.A.) and -35°27' Declination (Decl.)(NASA/IPAC Extragalactic Database). Apart from the central region, the Fornax Cluster also contains a subcluster centred three degrees to the South West with respect to the centre (Drinkwater et al., 2001). This subcluster includes the active lenticular galaxy NGC 1316, Fornax A.

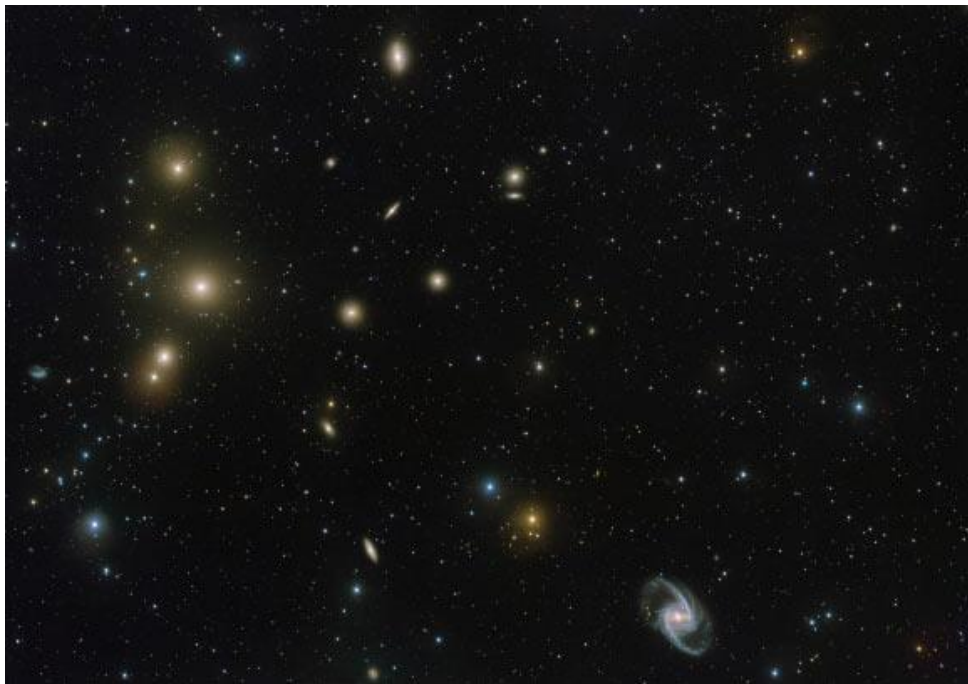


Figure 1.1: This VST image shows the central part of the Fornax Galaxy Cluster in great detail.  
Image credit: ESO / FDS

#### FDS<sup>2</sup>

The Fornax Deep Survey (FDS) is a deep multi-imaging survey of the Fornax cluster. The survey covers an area of approximately 30 square degrees around the cluster's central galaxy NGC1399. The FDS observations took place from 2012 to 2017 and were conducted with the OmegaCam on the VLT Survey Telescope (VST) (Venhola et al. 2018). The survey was taken in multiple bands, i.e. the u, g, r and i-band. In this project pre-processed FDS data from <http://www.astro.rug.nl/~fds/data.html> is

<sup>1</sup> Here after mentioned as the catalogue.

<sup>2</sup> <http://www.astro.rug.nl/~peletier/fds/>

used, which is also available on the ESO science archive. This data has been rebinned to a pixel scale of 0.2 arcsec. Figure 1.2 shows the area covered by the survey and the tiles into which it has been rebinned. As can be seen on the figure, tile 11 covers the centre of the cluster and contains the most labelled dwarf galaxies. A downside to tile 11 is that it also contains several bright stars, which can make it difficult to properly reduce the background, this will be further discussed in chapter 2.

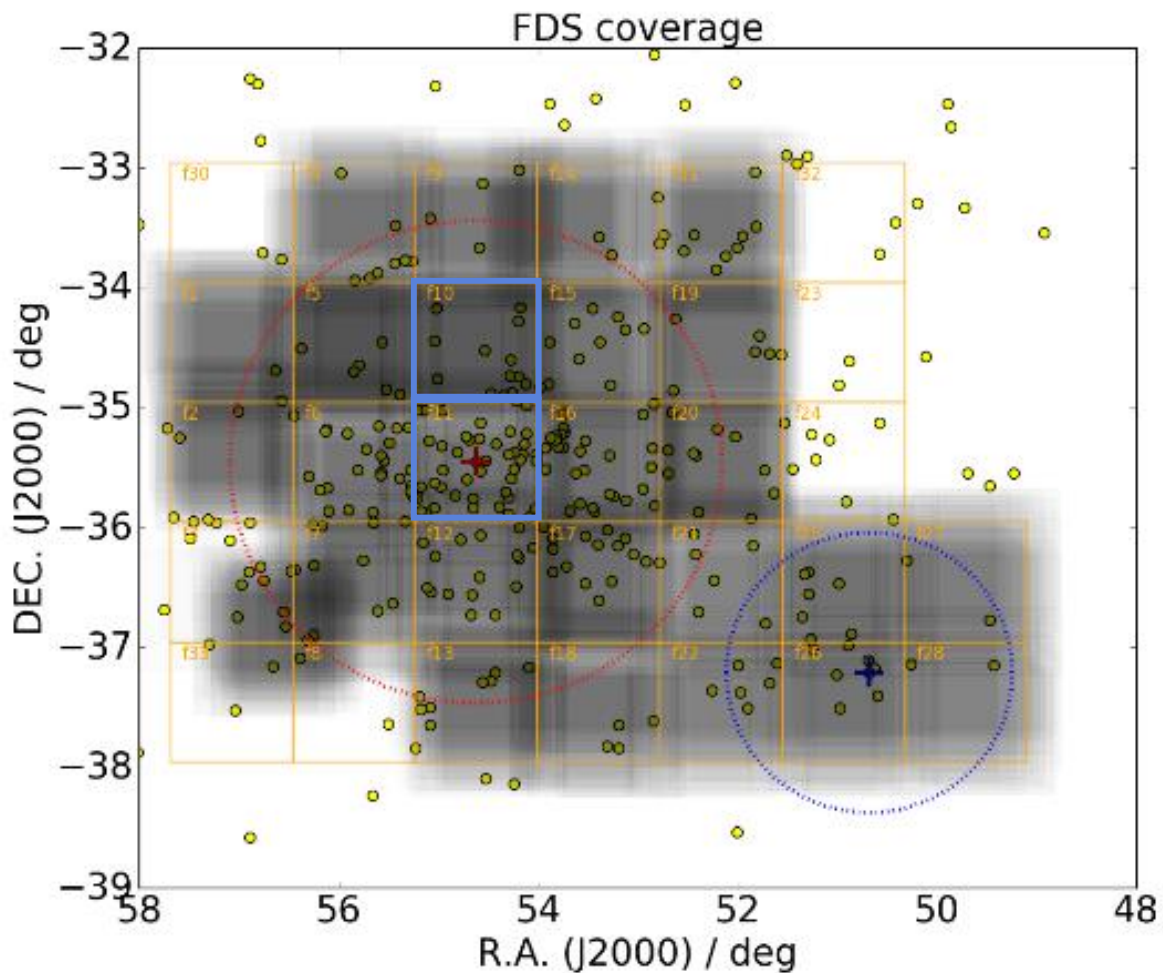


Figure 1.2:  $g'$ -band FDS coverage. Figure credit: Venhola et al. (2018) In this project tiles 10 and 11, marked by the blue squares, are used.

### NGC1427A

NGC1427A is the brightest dwarf irregular in the Fornax cluster, located near the centre of the cluster at R.A. 3h 40m 3.9s and Decl.  $-35^{\circ} 37' 28''$  (NASA/IPAC Extragalactic Database). In the catalogue, NGC1427A is labelled FDS11\_DWARF519. Given that NGC1427A is one of the brightest and largest dwarfs in the Fornax cluster and the FDS data on NGC1427A has been analysed before by Lee-Waddell, et al (2018), (In this paper, figure 2: smoothed VST images of NGC1427A, clearly shows how the galaxy differs in each band, which is a useful reference when determining whether the rgb-images conserve the galaxy's morphological features properly.) ,this galaxy has been used to develop and test the initial scripts in the project. Figure 1.3 shows an image of NGC1427A taken by the Hubble telescope.



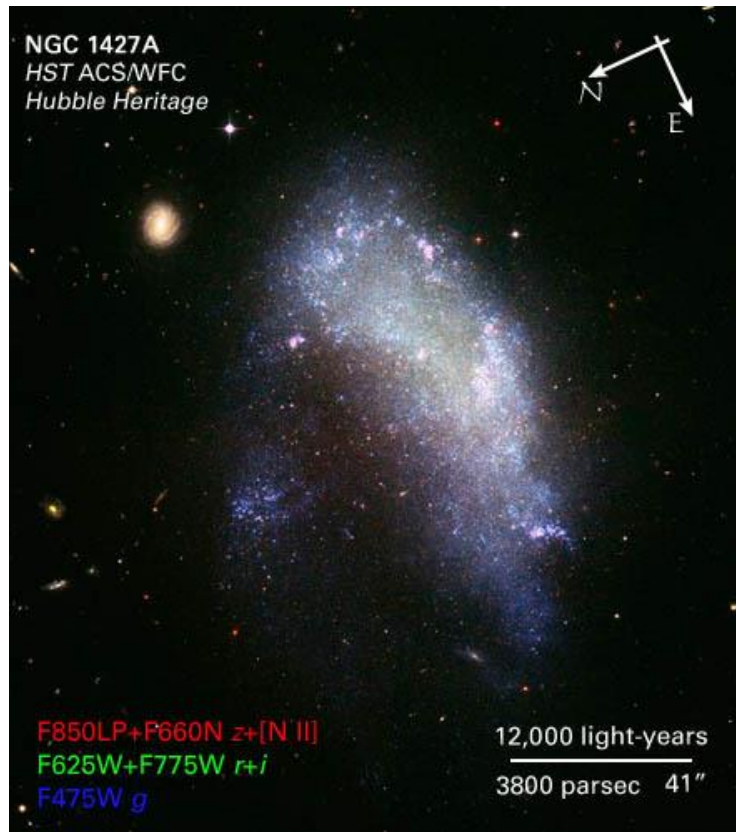


Figure 1.3: NGC 1427A image from Hubble data. Source: <https://hubblesite.org/contents/media/images/2005/09/1662-Image.html?news=true>

### VST and OmegaCAM

The FDS data was taken using the OmegaCAM on the VST. VST stands for VLT Survey Telescope. It is a 2.6 meter wide field optical modified Ritchey-Chretien alt-az survey telescope located in Chile. Detailed documentation on the VST and scientific research using VST and OmegaCAM data is provided by Arnaboldi et al. (1988) and Kuijken et al. (2002, 2011). The telescope operates in the optical, ranging from the u-band to the z-band. It is situated in Chile, at the ESO site in Paranal.

OmegaCAM is a wide-field imager for the Cassegrain focus of the VST. It allows the VST to observe in a 1x1 degree field of view, producing images 16x16 times larger than the Hubble telescope.<sup>3</sup> OmegaCAM can switch between 12 filters, including the Sloan ugriz set of filter of which the u-, g-, r- and i-band are used in this research. The main science goal of the VST OmegaCAM combination is to conduct very wide surveys in the optical range.

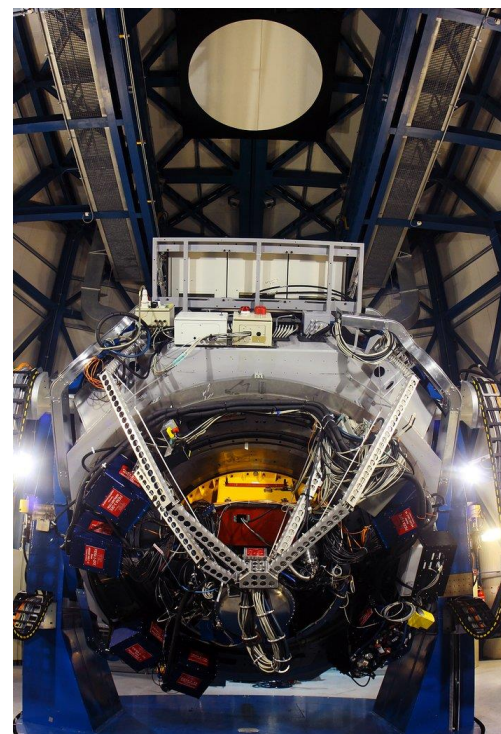


Figure 1.3: OmegaCam, credit: ESO

<sup>3</sup> <https://www.eso.org/public/teles-instr/paranal-observatory/surveytelescopes/vst/camera/>



## Chapter 2: Removing the background

Before the data can be transformed into colourful RGB's or be used to make accurate profiles, the background has to be reduced. Nearby sources, stellar halos on the foreground and random noise caused by the sky and the system all lower the accuracy and precision of the results, which is why an attempt will be made to minimize their impact.

### Dataset

The dataset used consists of .fits files from the FDS which were retrieved from <http://www.astro.rug.nl/~fds/data.html>, the cropped fits files from the April 2018 data release in the i-, r-, g- and u-band are used in this project. In the first stages of the project, i.e. ensuring the cropping of the FITS-files worked properly and testing several image processing programs, only the data on NGC1427A was used. In the next stages, the dataset was extended to the 52 dwarf galaxies in tile 11, whose morphology was indicated in the catalogue.

In the last stage of the project, developing the colour profiles, it was chosen to focus on a small subset of dwarf galaxies in tile 10. This is because there are fewer stars impacting the background for these galaxies. During development of the profile functions, the subset consisted of two dwarfs: FDS10\_DWARF023 and FDS10\_DWARF189. The final sample consisted of several dwarfs in tile 10, listed in appendix C, which were selected to cover a stellar mass range from circa  $10^6$ - $10^8$  solar masses. The mass of the dwarfs was determined using:

$$\log_{10} \left( \frac{M_*}{M_{\odot}} \right) = 1.04 + 0.817 * (g' - i') - 0.4 * M_r + 0.1 * (r' - i') \quad (2.1)$$

This formula for a stellar mass estimate has been derived from an empirical relation between the mass to light ratio and the g-i colour by Taylor et al. (2011), which has been adapted to this form by Venhola et al. (2019) such that solely depends on the variables available in the catalogue. The absolute magnitude in the r-band,  $M_r$ , is computed by subtracting 31.5 from the total apparent magnitude acquired from a sersic fit, which is given in the catalogue, as well as the values used to compute the g-i and r-i colours. The factor 31.5 was taken from Venhola et al. (2018).

### NGC1427A

To create RGB-images from the FDS data, it is first of all essential to be able to open and edit the FITS-files. Using NGC1427A to verify the code worked properly, a python script was developed which uses the coordinates and effective radius ( $r_{\text{eff}}$ ) (as defined in the Venhola et al. 2018 catalogue) of a dwarf galaxy to slice out a small square image with side of 20 times the effective radius. This factor was chosen because for this factor the entire dwarf galaxy is visible on the image and in case the data would be used for computation one can look up to 10 effective radii distance from the source.

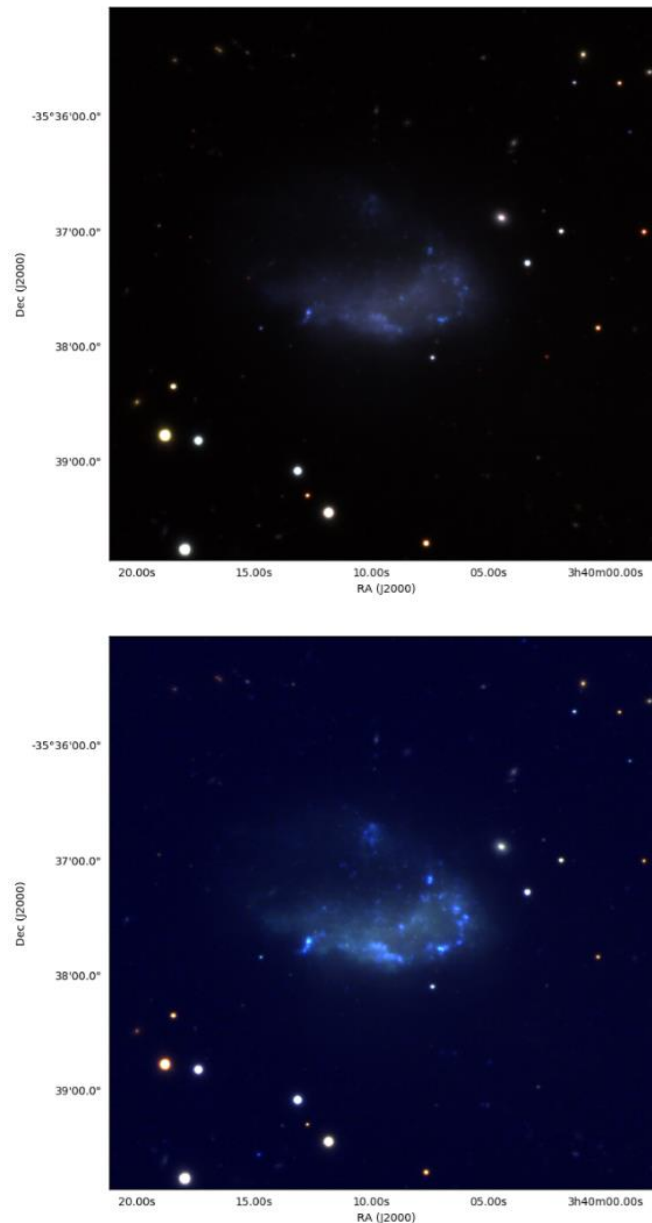


Figure 2.1 NGC147A\_rgb\_wcs\_gri (left) and NGC147A\_rgb\_wcs\_ugr (right) ESO science archive, Data from FDS (Venhola et al. 2018)

In the next step, programs to combine the FITS-files into RGB-images were explored. Sample ugr and gri images of NGC1427A were made using Astropy's `lupton_rgb`-function, Aladin and SAOImageDs9 (Ds9). Two pre-existing RGB-images of NGC1427A (Figure 2.1) and the more schematic figure in the Lee-Wadell, et al. (2018) paper (figure 6) were taken into consideration when creating the sample images. It was chosen to create a copy of the dataset in magnitudes per square arcsecond. This was done using  $[M = -2.5 \log_{10} F]^4$  where F is the pixel value. As upper magnitude 30 was chosen. This transformation changes the correspondence between intensity and colour, the look up table (LUT), and its limits in a way that makes outer regions, like the light red area in figure 2.2, more visible. It was chosen to continue the project making RGB's using SAODS9, partly because this program enables one to both adjust the value limits of each image separately and change the scale function and it can be accessed via the command line and thus be well-combined with the created python scripts.

<sup>4</sup>As mentioned on <http://www.astro.rug.nl/~fds/data.html>

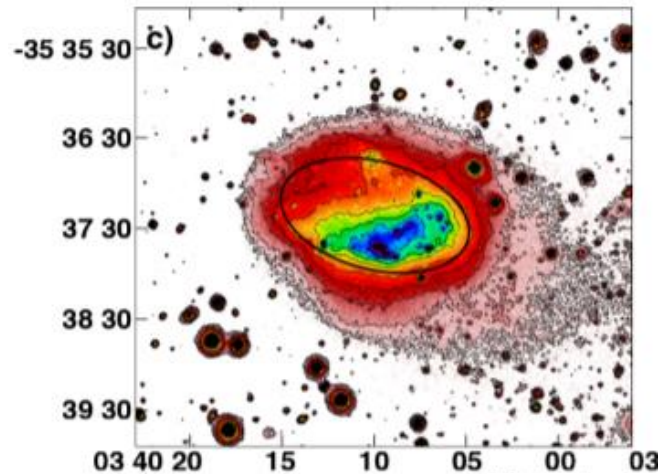


Figure 2.2: part of figure 2 from Lee-Wadell (2018). Compared to the other images used for reference, the outer regions of NGC1427A are clearly indicated here.

### Removing the background

The background in the initial data is not zero, even though scaled background frames have been subtracted during the reduction. This is because the sky varies with time. In addition, there are big differences between the bands causing RGB-images to have a non-black background. To solve this issue, the background has been corrected. Firstly the data was corrected by adding a constant and next the data was scaled by multiplying with a constant. These corrections were done using a grid oriented and histogram approach respectively.

#### Grid oriented

A script was developed to perform the linear correction automatically. If the absolute value of the median of the entire image is larger than  $1/10^{\text{th}}$  of the image's standard deviation (std), a factor chosen as very rough estimate of the standard deviation in the background, the background was corrected. The correction was done by adding/subtracting a constant which was determined sampling the median in small square regions, excluding the central  $16 * r_{\text{eff}} \times 16 * r_{\text{eff}}$  region. The mean value of all the sampled medians is taken and subtracted from the data. The central region was excluded to ensure that only the background and not the dwarf galaxy was sampled. The size of the sampling squares is  $1/100^{\text{th}}$  of the image size. Using the  $1/10^{\text{th}}$  std condition, all the u- and i-band FITS-files were corrected, in case of the g- and r-band correction was not always required.

#### Histogram approach

After the grid oriented background correction, the RGB-images still often displayed a blue rather than black background. Histograms were made of the data in all four bands to gain more insight into what further corrections were required. Figure 2.3 shows the histogram of FDS11\_DWARF277 before and after scaling. In the histograms, the peak of the histogram in all bands is approximately zero. This is in accordance with the linear correction done with the grid approach. The first histogram also shows that the broadness of the bands differs greatly. Especially the i- and the u-band curves are much broader than the g- and r-band. This is because the i- and u-band images are noisier. This difference was also visible on the histograms of the rest of the data. A program was made which rescales the i-, r- and u-band to the same width as the g-band curve. The aim of the rescaling is to reduce the effect of the large amount of noise in the i- and u-band on the rgb-image. Through the

rescaling, the data in all four bands has approximately the same amount of pixels with values close to zero (values corresponding to the background), which should result in a blacker, instead of clearly blue or red, background.

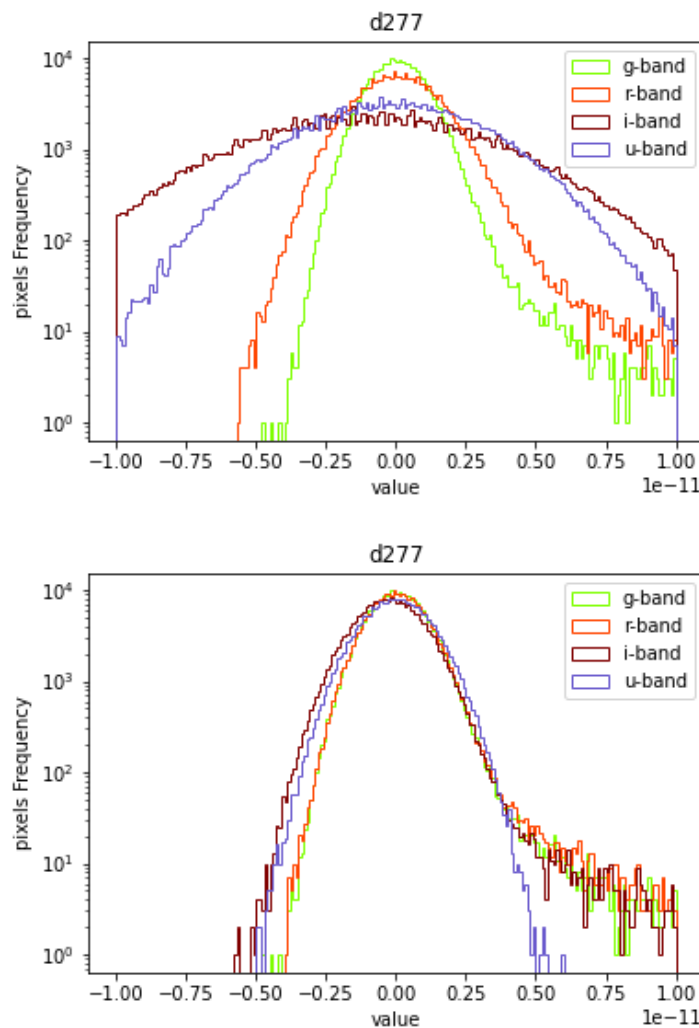


Figure 2.3: Histogram of FDS11\_DWARF277 before and after scaling

### Systematic noise estimate

As the histogram approach changes the relation of the intensity of the band with respect to each other, this method was not applied when creating the colour profiles. Only the grid oriented background reduction was applied in this case. Next, to estimate the error in the data, the standard deviation is sampled of various boxes located in the background. This estimates the systematic noise in the background. Noise of other non-systematic origin is not further investigated because it can be considered negligible compared to the systematic noise. The sample consists of several (>4) boxes of 5x5 pixels which by eye appeared to be empty. The standard deviation of the means of all boxes was taken as estimate of the systematic noise in the data. This value was found to be typically around  $10^{-14}$  for the g- and r-band and in the order of  $10^{-13}$  or even  $10^{-12}$  for the i- and u-band. This difference between the g-, r-band and i-, u-band is also noticeable by their difference in shape in the unscaled histogram.

### FDS-Band specific noise

The estimated error was found to be larger in the u-band because there are fewer photons in this range and the photons have a higher energy compared to the photons in the range of the other three bands.

The increased error in the i-band is due to fringing, see Rathi et al. (not yet published). The Silicon of the CCD becomes transparent as with increasing photon wavelength. I-band photons have a chance of passing through after which they can get reflected back, causing interference patterns. This sometimes amplifies, other times negates the original signal, resulting in fringe patterns as shown in figure 2.4. For the FDS data, there is not yet a straightforward way to fully correct for this.

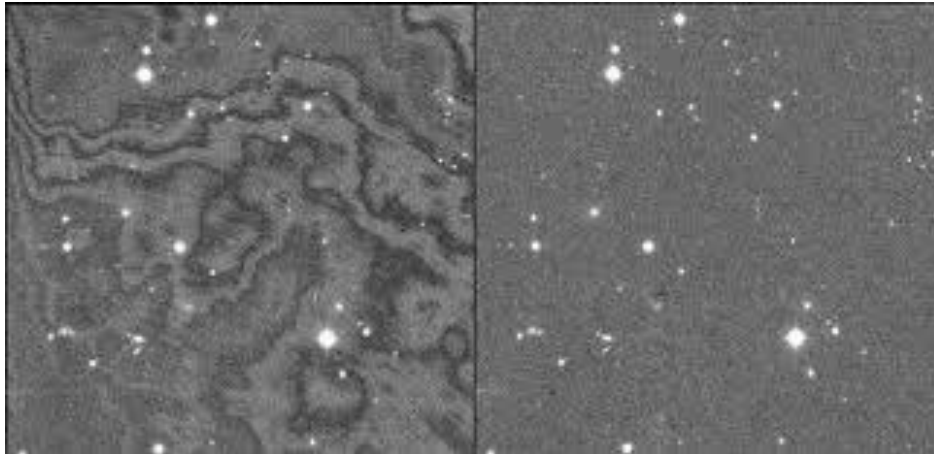


*Figure 2.4: A dataset with (left) and without (right) fringe-patterns.*  
Source: <https://www.astro.uni-bonn.de/theli/gui/aboutbackground.html>

Due to these additional effects in the i- and u-band, it was chosen to use the g-r colour profile when determining the difference Voronoi binning makes in the results.

### Masks

To filter out sources other than the dwarf galaxy of interest, when available, a mask was applied in the process of computing the colour profile. The masks are provided by Shivangee Rathi and made using MTOjects: the faint object detection method developed by Teeninga, Wilkinson and collaborators. See Haigh et al. (2021). The mask is zero for pixels that can be used and non-zero for those where other sources dominate, as shown in figure 2.5. The masked pixels are not used in the computation of the Voronoi tessellation or the colour profile.

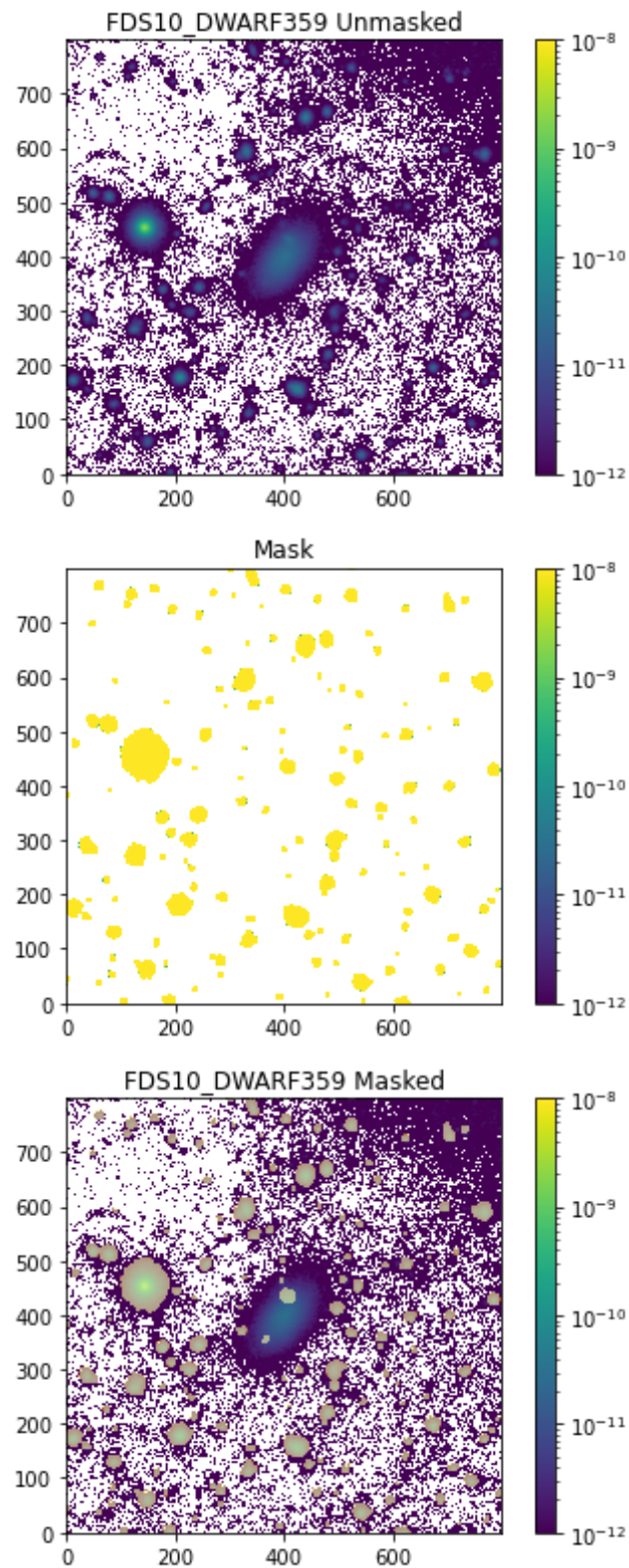


Figure 2.5: FDS10\_DWARF359 with and without a mask applied



### Chapter 3: Voronoi Binning

In order to determine the  $g - r$  colour of the dwarf galaxies in Fornax with a high accuracy, especially in the outer parts, it was chosen to apply Voronoi binning. Given a 2D dataset with the signal and noise of each datapoint, the `voronoi_2d_binning.py` function from the python package VorBin creates bins of data which meet a chosen minimum signal to noise ratio. Figure 3.1 provides an example of a dataset with and without Voronoi bins. (One can notice that the background in the Voronoi binned is less noisy.) In this chapter, the theory behind and the working of the Voronoi binning algorithm are explained.

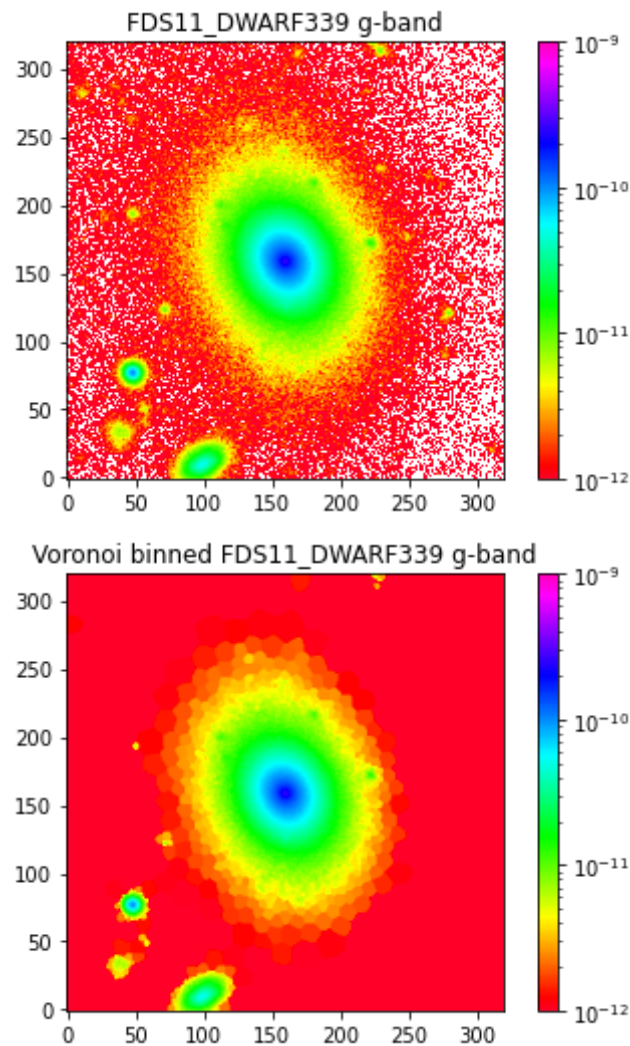


Figure 3.1:  $g$ -band image of FDS11\_DWARF339. Left: Unbinned, right: Voronoi binned (target S/N: 100). The scale and size of the images is the same. The axes indicate the pixels values of the image with the source centered at (170,170).

### Voronoi diagram<sup>5</sup>

A Voronoi diagram, or Voronoi Tessellation, is defined as *The partitioning of a plane with  $n$  points into convex polygons such that each polygon contains exactly one generating point and every point in a given polygon is closer to its generating point than to any other (Weisstein)*. The most simple case consists of several fixed points, seeds, where the Voronoi region of a seed contains all points which are closer to this seed than to any of the other seeds. The left image of figure 3.3 shows a Voronoi diagram where this case applies. Voronoi diagrams are named after the Ukrainian mathematician Georgy Voronoy, who was one of the first to formally introduce this concept. The concept has, however, already been around since the 17<sup>th</sup> century. The French philosopher Descartes uses a Voronoi diagram in his Principles of Philosophy, as shown in figure 3.2.

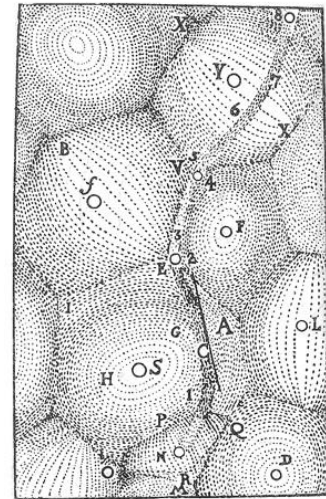


Figure 3.2: An old Voronoi diagram: *Plenum vortices in the Principles, Pr III 53 by Descartes in 1656 via <https://plato.stanford.edu/entries/descartes-physics/>*

There are generally two ways in which one can interpret the closest distance from a point to a seed: the Euclidian distance and the Manhattan distance. The Euclidian distance between two points,  $a$  and  $b$ , in an  $n$  dimensional space, is defined as:

$$d(\mathbf{a}, \mathbf{b}) = \sqrt{(a_1 - b_1)^2 + (a_2 - b_2)^2 + \dots + (a_n - b_n)^2} \quad 3.1$$

Here points  $a$  and  $b$  have cartesian coordinates  $(a_1, a_2, \dots, a_n)$  and  $(b_1, b_2, \dots, b_n)$ . The Manhattan distance, which is named after the grid like structure of the street plan in Manhattan, measures the rectilinear distance and is defined as:

$$d(\mathbf{a}, \mathbf{b}) = |a_1 - b_1| + |a_2 - b_2| + \dots + |a_n - b_n| \quad 3.2$$

Figure 3.4 illustrates the difference in the Voronoi diagram when these two ways of measuring distance are applied on the same dataset. In this project Voronoi bins will be created using the Euclidian distance.

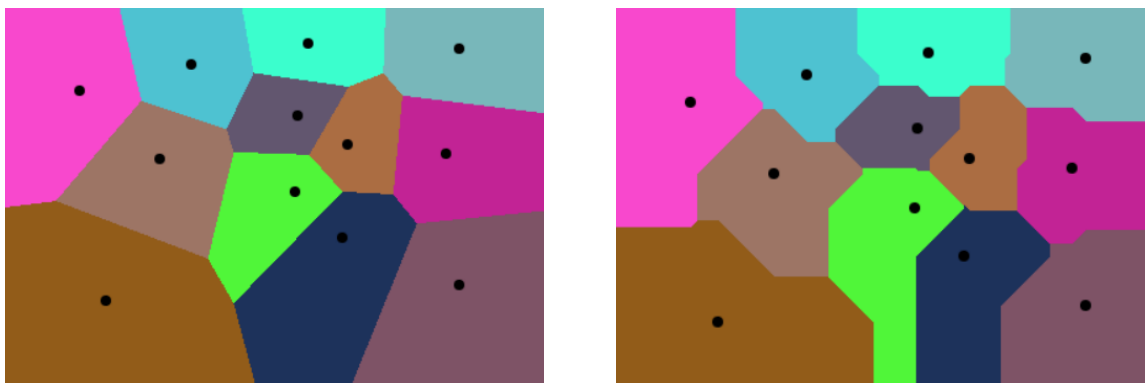


Figure 3.3: the Voronoi diagram of twelve points in a two-dimensional space. On the right, the Euclydian distance. On the left, the Manhattan distance. The diagrams were made using an online vsualisation program: <http://sygreer.com/projects/voronoi/>.

### Voronoi Binning

In this project, the possibilities of Voronoi binning were examined by applying the VorBin python package (developed by M. Cappellari) on the data. As described in detail by Cappellari, M. and Copin,

<sup>5</sup> Section based on Aurenhammer et al. (1999)

Y. (2003) , the aim of Voronoi binning is to bin a dataset such that each bin has the desired signal to noise. The input is a dataset consisting of x and y coordinates, pixel values, noise and the desired signal to noise. (In this project the noise was chosen to be a constant, the standard deviation of the pixel values divided by 50.) By binning two pixels which each have a signal to noise (S/N), the new signal to noise becomes:

$$\frac{S}{N_{1+2}} = \frac{S_1+S_2}{\sqrt{N_1^2+N_2^2}} \quad 3.3$$

One can easily bin pixels in 1D to get the desired signal to noise, yet in 2D it is difficult to determine which pixels are best binned together. Voronoi binning provides a solution for this by creating Voronoi diagram like bins. The VorBin algorithm starts by creating the first bin containing the pixel with the highest S/N. The mass centroid of the bin is computed and the unbinned pixel closest to the centroid is selected as new candidate for the bin. Next the algorithm checks whether the three conditions for good binning (mentioned in section 1 of the paper) are met. The three conditions are:

1. **Topological:** Are the new pixel and the current pixel adjacent?
2. **Morphological:** Is the bin as compact as possible and therefore round enough? (The roundness is, as defined by the author of the paper,  $r_{\max}/r_{\text{eff}} - 1$ , where  $r_{\max}$  is the maximum distance between the centroid of the bin and any of the bin pixels, and  $r_{\text{eff}}$  is the radius of a disk of same area as the whole bin. The author's found that 0.3 is a good upper limit for the roundness.)
3. **Uniformity:** Is the scatter in the S/N minimized? Addition of the new pixel should not make the S/N of the bin deviate more from the target S/N than before, if the bin S/N is already close to the target value.

If these three criteria are fulfilled, the candidate pixel is appended to the bin and the next pixel is examined. Once this process has come to an end, it is examined whether the uniformity criterion is met. If the criterion is met all pixels are labelled 'successfully binned', otherwise they are labelled 'unsuccessfully binned'. In the following step, the mass centroid of all of the already binned pixels is evaluated and a new bin is started from the unbinned pixel closest to it, the earlier steps are repeated for this new bin and the process continues until all pixels are binned. Next, the centroids of the successful bins are computed and the unsuccessfully binned pixels are reassigned to the closest of the centroids. In the last steps, the centroids of each of the bins are recomputed and used as initial generators for a Central Voronoi Tessellation (CVT). The CVT is computed using a modified Lloyd method. Cappellari and Copin mention that this method has two main practical limitations: Firstly, the modified Lloyd method does not guarantee that all the bins have equal S/N and secondly, the method does not work well when the bins consist of just a few pixels.

The output consists of a list of the bins to which each datapoint has been assigned and, if plot is set True, a plot similar to figure 3.4, which consists of a map of the Voronoi bins and an overview of the S/N of the bins with respect to the target S/N.

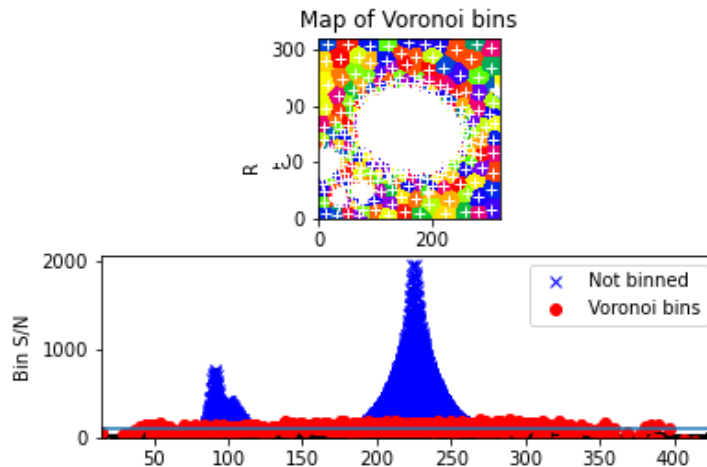


Figure 3.4: The plot-output when running `voronoi_2d_binning.py` on the dataset of FDS11\_DWARF339 with a target S/N of 100 and applying CVT.

## WVT

The above method uses the centroids of the bins to create the final Voronoi diagram, this is known as a CVT. In a CVT the bin to which a pixel belongs is determined by finding for which bin the pixel has the shortest distance to the centroid (generator). This definition can be made more flexible by adding a scale length to each of the bins and finding the bin for which the pixel has the shortest distance to the generator divided by the scale length, which results in a Voronoi diagram with rounder bins. This results in a WVT or Weighted Voronoi Tessellation. This method has been described by Diehl, S. and Statler, T. S. in *Adaptive binning of X-ray data with weighted Voronoi tessellations*. The authors mention that WVT can be applied to a wider range of datasets than CVT, and show by applying both methods to the same data set, WVT results in a Voronoi diagram with consistently rounder bins. The WVT method consists of 5 steps:

1. Start with an initial WVT
2. The S/N, area and centroids (as initial generators) for each bin are evaluated
3. The scale length for each bin is computed, using:

$$\text{scalelength} = \sqrt{\frac{\text{Area}}{\text{constant}} \cdot \frac{\text{target S/N}}{\text{S/N}}^{3.4}}$$

4. All pixels are reassigned to a new WVT with the computed generators and scale lengths.
5. The process is repeated from step 2. until the bins no longer change significantly.

The VorBin package has the option to use WVT instead of CVT. In this research WVT will be used. Figure 3.5 illustrates shows the plot output when WVT is selected, whilst the other variables remain the same as the input for figure 3.4. Figure 3.6 shows the difference between the two algorithms in the g-r diagram of FDS11\_DWARF339. The WVT-version clearly has rounder bins.

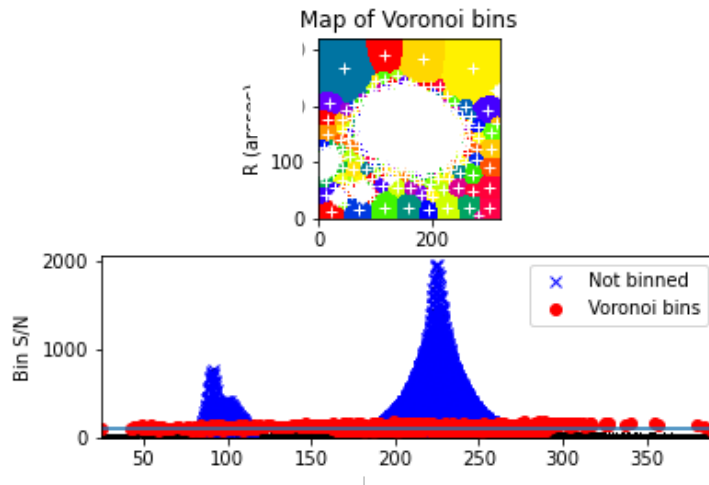


Figure 3.5: The plot-output when running `voronoi_2d_binning.py` on the dataset of `FDS11_DWARF339` with a target S/N of 100 and applying WVT.

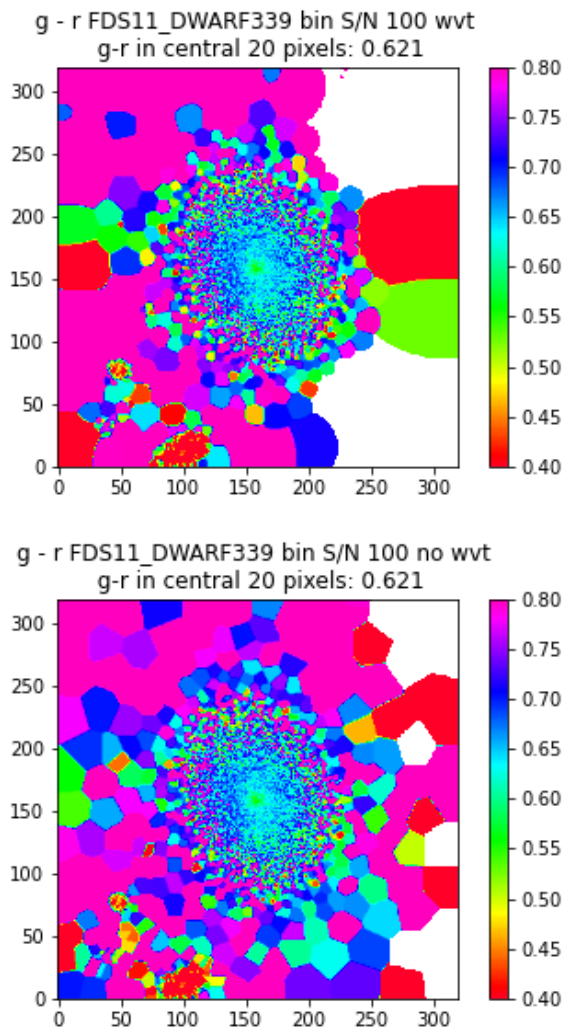


Figure 3.6: *g-r* colour diagram of `FDS11_DWARF339`. On the left: weighted Voronoi tessellation. On the right: Central Voronoi tessellation. The target S/N was set to 100 in both cases.

## Chapter 4: colour profiles and RGB images

This chapter is centred around colour. First, the importance and creation of colour profiles is discussed, which provides a relevant background for the results shown in chapter 7. Next, the process of creating RGB-images from multi-band data is investigated, which underlies the method behind the RGB-images presented in chapter 6.

### Colour

The colour of regions in a galaxy provides information about their stellar population, which is the composition of the stars and their ages. The combination of stars in a region determines its colour. Generally, in young regions, the light from newly formed bright hot, blue, stars dominates, resulting in a region that appears bluer. In older regions, the blue stars have depleted their fuel and the cool, red, stars dominate, resulting in regions that appear red.

If one were to make colour profiles including a band covering the infrared, one can also deduce information about the spread of dust in a galaxy and whether the redness in a region is primarily due to dust or a lack of young blue stars (Peletier et al. 1999).

Colour profiles are thus useful to determine the age and metallicity of regions within galaxies. These factors are relevant when unravelling a galaxy's specific star formation rate. Studying colour is also interesting because it is affected differently than e.g. a galaxy's morphology by environmental effects. The results of Blanton et al. (2005) imply that a galaxy's mass and colours are more closely related to galaxy environment than its structural properties.

### Colour computation

Given datasets of the flux in the g and r band ( $F_g$  and  $F_r$ ), the g-r colour is obtained using:

$$g - r = -2.5 \log_{10}(F_g) + 2.5 \log_{10}(F_r) = -2.5 \log_{10}\left(\frac{F_g}{F_r}\right) = 2.5 \log_{10}\left(\frac{F_r}{F_g}\right) \quad (4.1)$$

To determine the colour profile of a dwarf, it is common to sample g-r in circular or elliptical rings. The steps for creating a colour profile are as follows:

1. Divide the dataset into rings (shaped like the source), centred around the centre of the source.
2. Compute the mean value of the flux in both bands in each of the rings.
3. Compute g-r for the values found in step 2, using formula 4.1.
4. Make a plot of the g-r values against distance from the source.

In addition one can compute the error in g-r using the error propagation provided in the *Error Propagation*, at the last page of this report. In the computation, a pre-estimated systematic uncertainty in the value of the background in both bands and the mean values from step 2 are used.

### RGB image creation

The VST collects data for the FDS in the i-, r-, g- and u-band on the SDSS system. These bands are centred around 770, 625, 480 and 350 nm respectively (Fukugita et al 1996). The human eye is sensitive to a region from approximately 750 -380 nm, ranging from red to violet. As the bands do not coincide with the human perception of colour, this chapter will address how one can transform multiband datasets into RGB-images whilst maintaining most of the data's original characteristics.

RGB stands for Red, Green, Blue. It is a colour model that uses these three colours as basis and uses additive colour mixing to form other colours. (Additive colour mixing means that, like with light, all colours together result in white.)



## The use of Voronoi binning in obtaining Colour profiles of FDS dwarfs

The RGB images are made by colours to the bands and subsequently combining these single colour images into one multicoloured one. Figure 4.1 demonstrates this process. It is the norm to assign colours in a fixed chromatic order: starting with blue being assigned to the band with the highest wavelength and ending with assigning red to the lowest wavelength band.

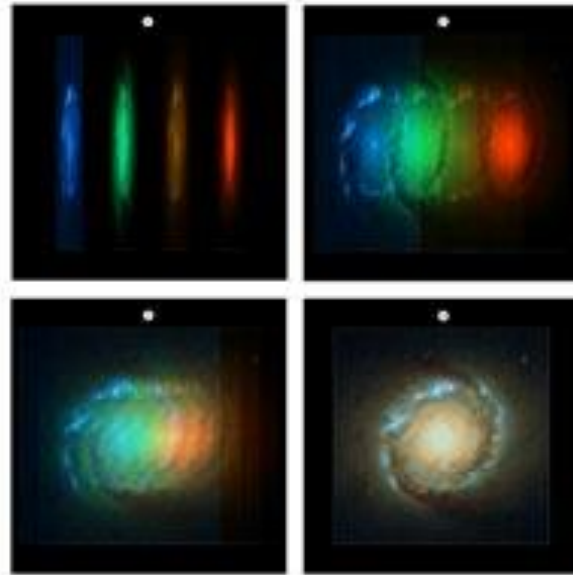


Figure 4.1: From esahubble.org. Illustrates how colour images are made

After the bands have been assigned to colours, the image can be fine-tuned by adjusting the scale function, limits and optional other effects like smoothing. As long as one pays attention that the image stays scientifically accurate, e.g. the chromatic order is not broken, this process is generally a matter of aesthetics. By picking a different scale function, one can highlight different elements of the dwarf galaxy. Figure 4.2 demonstrates the difference between the linear and logarithmic source function.

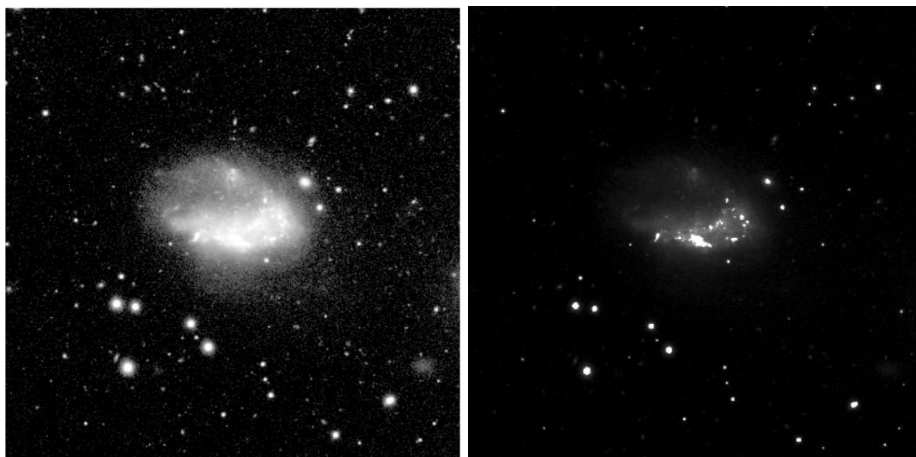


Figure 4.2: g-band image of FDS11\_DWARF591 with a linear(left) and logarithmic(right) source function

## Methods

### Chapter 5: Computations

#### The process

In this chapter, the data processing is described in a stepwise manner. The generalised version of the codes created are provided in Appendix E.

In order to create profiles of the colour of a dwarf galaxy from FDS data, the following steps were taken:

#### Step 1: Acquiring the data

.fz-files containing pre-processed FDS data of the tiles shown in figure 1.2 were obtained from <http://www.astro.rug.nl/~fds/data.html>. Using the funpack function from Cfitsio, the .fz were converted to .fits, a file type that can be handled in Python using the AstroPy package.

Next, using the coordinates and effective radius provided by the catalogue, smaller datasets are sliced from the tile data. The algorithm Table2Tile, shown in Appendix C1, takes the tile fits-files and a list of dwarf galaxies with a R.A., Dec. and effective radius and outputs images with a size of  $20 * r_{\text{eff}} \times 20 * r_{\text{eff}}$  in all four bands of all the listed dwarfs. These images are saved at a given location in both the original units and in a version in magnitudes per square arcsecond. The latter is used for the creation of RGB-images. The upper limit of the version in magnitudes is set to 30.

#### Step 2: Background reduction

During the pre-processing of the data, sometimes the sky was over or under subtracted. To correct for this, the algorithm also samples the median and standard deviation of the data in boxes at the outer 2 effective radii of each images. The box size is  $100^{\text{th}}$  of the image size (rounded to an integer), unless the image is smaller than  $100 \times 100$  pixels, in which case it is set to  $9 \times 9$  pixels. We use the median of the median values in these boxes. If the absolute value of this exceeds  $1/10^{\text{th}}$  of the standard deviation, the data is corrected by subtracting this median. It was chosen to use the median to minimize the impact of sampled boxes that happen to contain bright background objects.

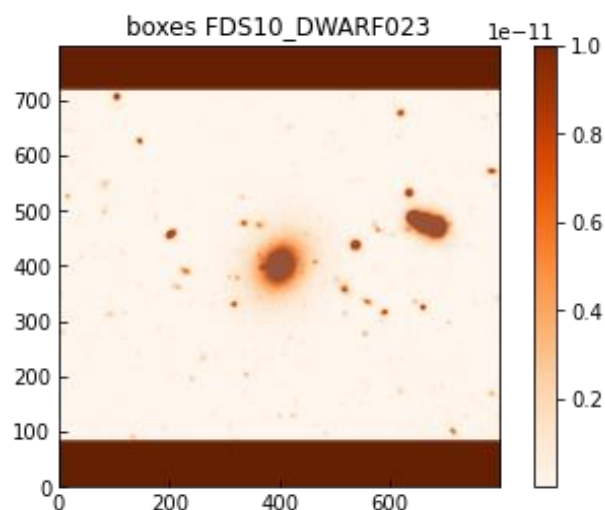


Figure 5.1: Overview of the sampled boxes: The dark areas at the top and bottom contain 1900 boxes of  $8 \times 8$  pixels which are used to sample the uncertainty in the background for FDS10\_DWARF023

The following steps focus on the processing of the data for the results presented in chapter 8. For the creation of the several series of RGB images presented in chapter 6, only steps 1 and 2 apply, were mentioned in addition with histogram scaling, as explained in chapter 2, and further processing in SAODS9.

### Step 3: Voronoi binning

Using the linearly background corrected galaxy cut-outs, lists are made which contain the x- and y-coordinates, the signal, which is the pixel values, and a noise constant. The noise constant was chosen to be the standard deviation of the cut-out divided by a factor of 100. This list serves as the input for the VorBin algorithm, which is detailed in chapter 3. Both the choice of noise constant and target signal to noise ratio affect the size of the bin and the distance at which the binning starts. It was chosen to set the noise constant to a small value, such that a wide range of target signal to noise values could be tested using the same list. The target signal to noise is, unless otherwise mentioned, set to 100, as this resulted into a distribution of bins where the centre was mostly unbinned, whilst the outskirts consisted of increasingly larger bins in all the datasets that were tested. Appendix A, demonstrates this by showing how the distribution of bins changes for the g-r plot of FDS11\_DWARF339 when the target signal to noise in the VorBin algorithm is set to values ranging from 10 to 9000. Next, the output list of bins is applied on the dataset: the median of all pixels belonging to the same bin is computed and replaces the value of those pixels.

In case a mask, as detailed in chapter 2, was available, this is applied when creating the table for Voronoi binning. Doing so foreground or background sources are not taken into account when creating the bins, which results in a cleaner signal. Figure 5.2 illustrates the difference between applying and not applying a mask. The amount of unbinned areas outside of the central source is clearly smaller and the size of the bins further away from the source has increased.

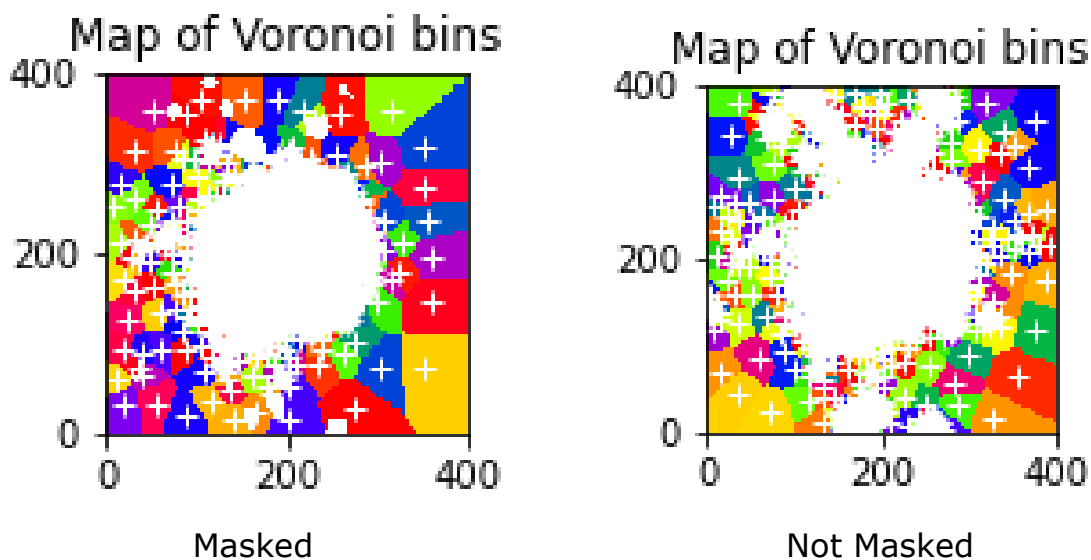


Figure 5.2: On the right: Map of the Voronoi bins of FDS10\_DWARF023 (g-band) with the mask applied. On the left: the same map without the mask applied.

### Step 4: Making the profile

In order to create the g-r colour profile of a dwarf, firstly the average value of the g and r data is computed in rings. These outer radius of each ring is defined as a fraction of the effective radius. In case it was available, a mask is applied. Depending on the ellipticity of the galaxy, which is provided in the catalogue and can also be estimated by eye, the rings are either spherical or elliptical. Both functions will be described.

*Spherical profile sampling*

When the profile is made using spherical rings, first a list of radial bin limits is created, starting with zero. Next, the mean value of all (unmasked) pixels that are within the current radial bin limit (excluding zero) but outside of the previous one is determined and appended to a list. This process is done in all four bands. The intensity weighted average radius in each ring is computed using:

$$\bar{r} = \frac{\sum_i r_i I_i}{\sum_i I_i} \quad (5.1)$$

Where I is the intensity, which was chosen to be the intensity of the pixels in the r-band when creating the g-r profile.

*Elliptical profile sampling*

Apart from a list of radial bin limits of the x axis, this method also required the ratio between the minor and major axis of the ellipse and the angle by which the ellipse is rotated as input. The ratio is provided in the Venhola et al. (2018) catalogue as *arat*. The angle is measured by hand. Instead of a radius based condition, this method uses the definition for points on an ellipse:

$$\frac{x^2}{a^2} + \frac{y^2}{b^2} = 1 \quad (5.2)$$

Arat is used to determine the ratio between a and b, and a, the semi major axis, is a distance that increases according to the input list of distances, the equivalent of r in the spherical version. When the ellipse is rotated by an angle  $\theta$ , this becomes:

$$\frac{(x \cos(\theta) - y \sin(\theta))^2}{a^2} + \frac{(x \sin(\theta) + y \cos(\theta))^2}{b^2} = 1 \quad (5.3)$$

When selecting the pixels belonging to a ring with outer maximum radius of  $a$  and inner radius of  $q$ , the criteria are that the left handed side of function 5.3 must be equal to or smaller than 1 for  $a$  but larger than 1 for  $q$ . This is demonstrated in figure 5.3, where a and q are chosen to be [10,1], [100,50] and [300,250].

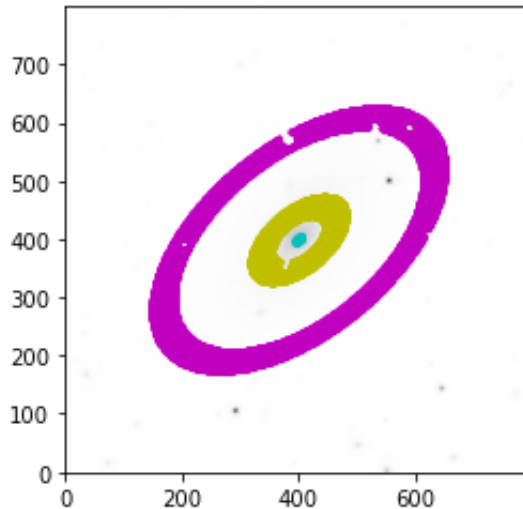


Figure 5.3: Elliptical rings on Masked FDS10\_DWARF189. The bins were created with the elliptical profile sampling function. The blue bin contains the pixels with the ellipse with a maximum radius of 10 pixels (outer maximum), but outside the ellipse with a maximum radius of 1 pixel (inner maximum). In the yellow bin the inner and outer maximum radii are 50 and 100 pixels respectively. In the magenta bin, the inner and outer maximum radii are 250 and 300 pixels.

Next, the colours are computed for the mean value of each ring. This is done using function 4.1. Although apart from g-r, colours like r-i and u-g were computed as well, it was chosen to only use the g-r profile when determining whether Voronoi binning improves the range up to which one can accurately determine the colour, due to the large errors in the i- and u-band.

### Step 5: The error

Finally, the error is computed. For two fluxes in different bands,  $F_g$  and  $F_r$ , this is done using the formula:

$$\Delta_{g-r} = 1.08574 \sqrt{\left(\frac{\Delta F_r}{F_r}\right)^2 + \left(\frac{\Delta F_g}{F_g}\right)^2} \quad (5.4)$$

The derivation of this formula is shown in the error propagation. The error is computed using the mean values per ring acquired in the previous step and using estimates of the systematic uncertainty. These estimates are done by manually selecting several regions of the dataset that appear to contain only background and determining the mean value of small (e.g. 10x10 pixels) subareas within these regions. The standard deviation of these values is taken as the systematic uncertainty estimate. The estimated error is usually around the order of  $10^{-14}$  up to  $10^{-13}$ , where the i- and u-band error are clearly larger than the error in the g- and r-band. It was chosen to only sample the systematic error because errors caused by other means are highly likely to be of a smaller magnitude than the systematic error, as explained in chapter 2. Because of these reasons it was chosen to focus on the g-r colour.

Using the error in the colour, the final profile, now with error margins, is plotted. In addition a plot is made where the error of the Voronoi binned and not Voronoi binned, hereafter referred to as unbinned, version are compared.

## Results

### Chapter 6: RGB image results

This section consists of a brief list containing the settings and details of the series of RGB-images made from the FDS-data. Appendix B contains an overview of the images in the final series of tile 11 gri-images. In this chapter, general information on the produced series of images as well as a description of the final series of images is provided. Appendix D contains a description of series 0-5.

### Filenames

The name of each dwarf galaxy has been abbreviated to 'd#' in the filenames, where # stands for the number in the galaxy's original name. For convenience, a generalized filename for images in a series has been included in the title of the section on that series below. As all galaxies used in this phase of the project belong to tile 11, FDS11 has not been included to the filenames. The order of the letters, i.e. ugr or gri, indicates which colour represents that filter in the image. The first letter is blue, the second green and the last red. For example, if an image has a filename ds9\_d339\_ugr\_log.png, it is an rgb image of the dwarf galaxy FDS11\_DWARF339 made from the logarithmic fits files which were combined in ds9 where the r-band is red, the g-band green and the u-band blue. As some galaxies have a bright source nearby, a very high magnitude or a background with a strong gradient, sometimes the prefix 'source' or 'faint' was added to the filename. To create optimal RGB-images of these galaxies requires performing some additional adjustments. A clear example of an uneven background due to a bright nearby source is shown below in figure 6.1. This galaxy has been studied in detail by Mentz et al. (2016).



Figure 6.1: Source\_aladin\_d235\_ugr\_log.png

### Series 6: colour differences per filter (autod#/ds9\_ugr\_realistic.png)

This final series was made to make the images appear more realistic. (i.e. more white instead of yellow or green as in series 3,4,5, which are presented in appendix D) To achieve this, the limiting values were adjusted per filter. The logarithmic fits files were used and the scale function is LINEAR. The upper limit of each filter was chosen to be 29.992, in order to exclude the background at 30. In the ugr-image the lower limit for the r-band is 25.7001, g-band 24.8731 and u-band 26.7069. In the gri-image the i-band has a lower limit of 26.9201, the r-band 25.5675 and the g-band 25.1744. NGC1427A was used to determine the limits. The ugr-images now look more orange than yellow and the gri-images are no longer green.



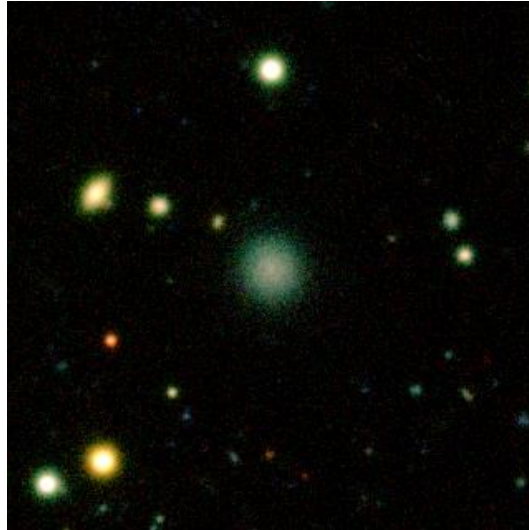


Figure 6.2: *autod47/ds9\_gri\_realistic.png*

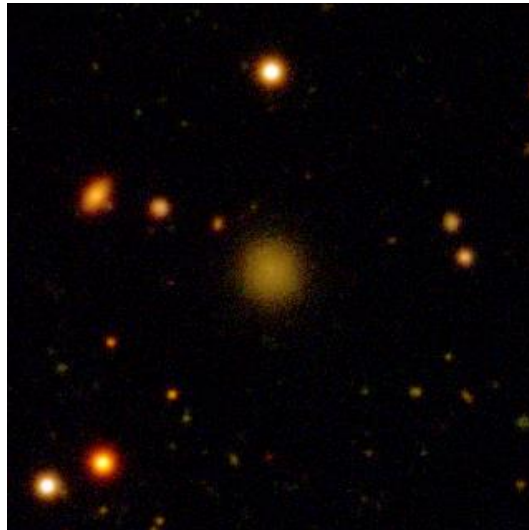


Figure 6.3: *autod47/ds9\_ugr/realistic.png*

## Chapter 7: Research Results

The results for each of the dwarf galaxies are presented below. Tables with the numerical output, location, input parameters and a g-band image of each of the dwarf galaxies are provided in appendix C. This appendix also contains the stellar mass estimates and apparent r-band magnitude within 1 effective radius, to give an indication of the differences in mass and brightness between the various dwarf galaxies investigated.

### FDS10\_DWARF023

As mentioned in chapter 2, due to the larger errors in the u-band and i-band, only the g-r profile will be computed and investigated. To determine whether this assumption was indeed justified, a profile of FDS10\_DWARF023 was made in each of the four bands. As one can see in figure 7.1, the uncertainty in the i-band does indeed blow up at a smaller radii than the g- and r-band. The u-band also increases in uncertainty at a shorter distance, which is to be expected as it begins at a higher magnitude, close to 28, than it does in the other bands.

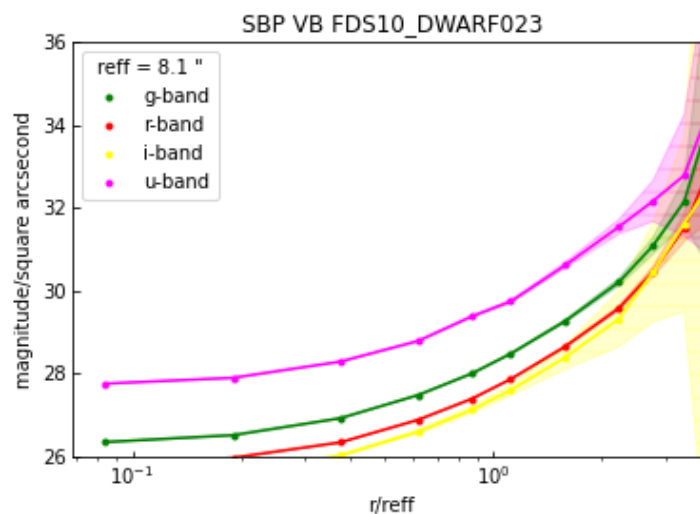


Figure 7.1: The value and uncertainty in magnitude per square arcsecond in all four bands. The dots indicate the weighted radial distance of each ring from the centre of the dwarf, as explained in chapter 5.

In figure 7.2, the g-r colour profile of FDS10\_DWARF023 is presented for the version with and without Voronoi binning. Due to the availability of a mask, it was possible to filter out the largest background sources and thus determine the colour profile with relatively little contamination except for the systematic background noise.

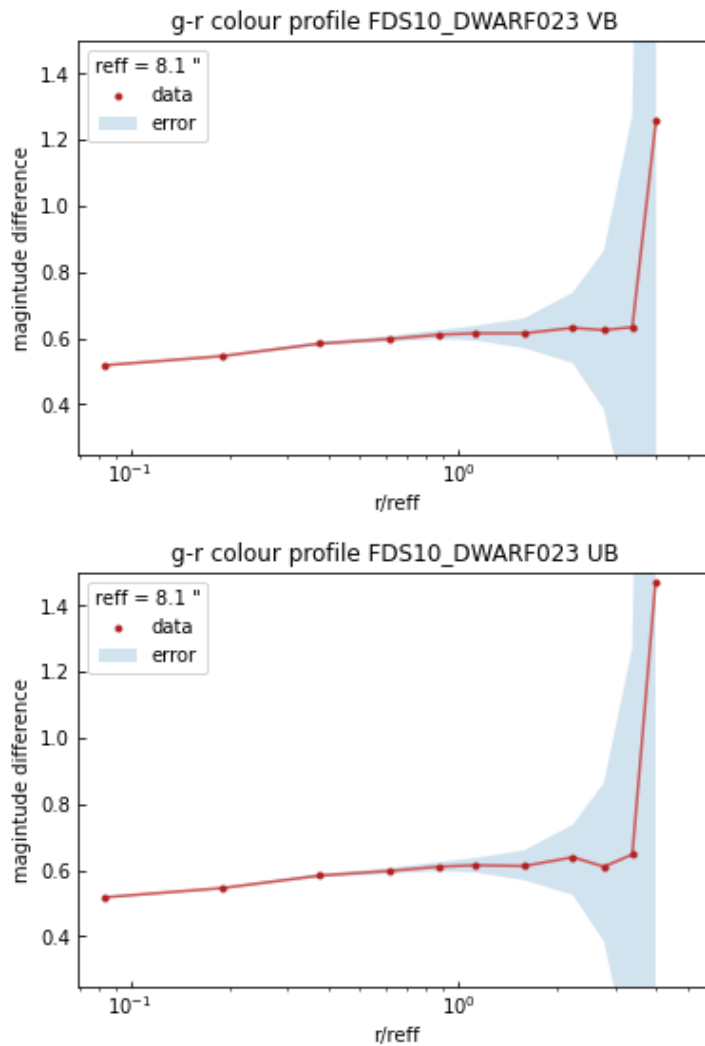


Figure 7.2: *g-r* profile of FDS10\_DWARF023 Voronoi binned (top), unbinned (bottom)

As is shown in the profiles, both the Voronoi binned and unbinned version agree on the *g-r* colour within the first several effective radii. Within the effective radius, both profiles rise from a colour difference between 0.5 and 0.6 to one slightly over 0.6. The mean value within 1 effective radius was found to be 0.579 for the unbinned and 0.578 for the Voronoi binned version, both with an uncertainty of 0.01. Using the Venhola (2018) catalogue values, one finds *g-r* to be  $0.583 \pm 0.05$  within 1 effective radius. All three values overlap within the margin of error.

Moving further away from the centre, the surface brightness lowers, which causes the error margin to increase. This is visible in the profiles. At more than 2.5 effective radii, both profiles begin to drop slightly, rise, drop back and finally steeply increase. After circa 3.5 effective radii, both errors begin to increase to sizes larger than the colour value itself. Figure 7.3 shows how the size of the error (magnitude) increases as the effective radius increases. Notice how the unbinned error jumps to extremely large values at 4 effective radii, whilst in the Voronoi binned version, this jump takes place around 4.5 effective radii.

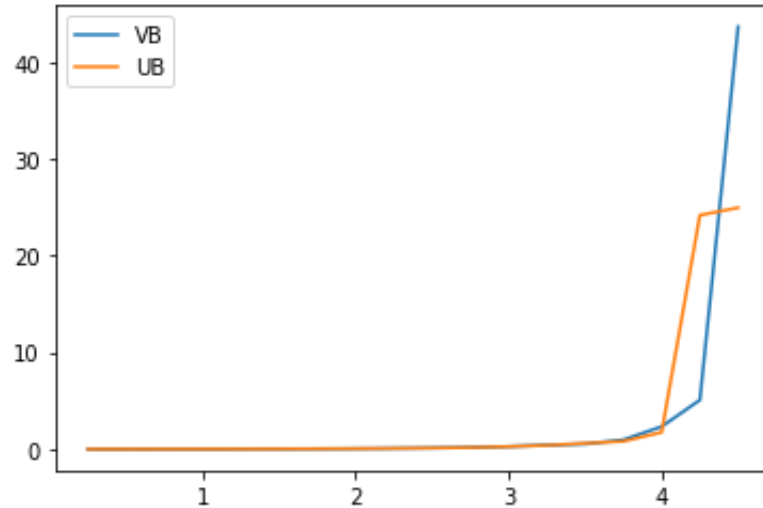


Figure 7.3: The uncertainty in the g-r profile of FDS10\_DWARF023, notice how the uncertainty in the Voronoi binned version increases at a slightly larger distance than the unbinned version.

The further one moves away from the source, the weaker the signal gets, up to the point where the noise begins to dominate. At these distances, the signal will begin to fluctuate around zero and the outputted g-band or r-band signal may be negative, which, when applying formula 4.1, would result in a negative log that does not exist. As the uncertainty is already several factors larger than the signal when this happens, it was chosen to set the radial limit of the presented g-r profiles to just before this phenomenon occurs.

To give an indication of the total area covered when computing the profile and the values masked, figure 7.4 gives an overview of the covered field, in turquoise, and the masked values, in olive green/cream. This applies to both versions. In addition figure 7.5 shows the difference in g-r plot for both the Voronoi and unbinned version.

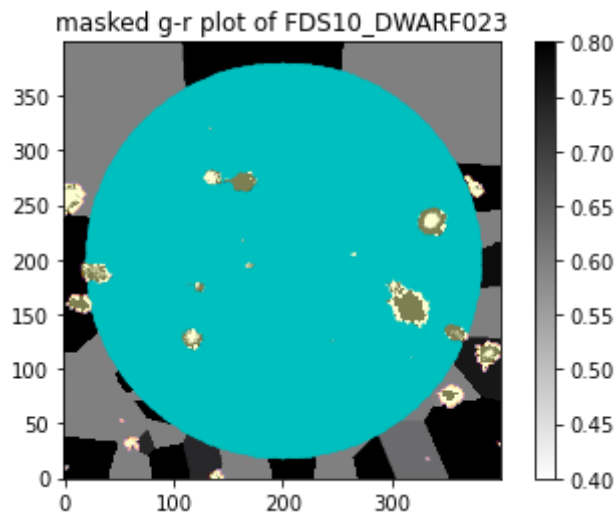


Figure 7.4: A map of the datapoints used in the profile creation (turquoise). The olive and cream spots are covered by the mask and thus excluded from the calculations. 1 effective radius corresponds to 40 pixels.

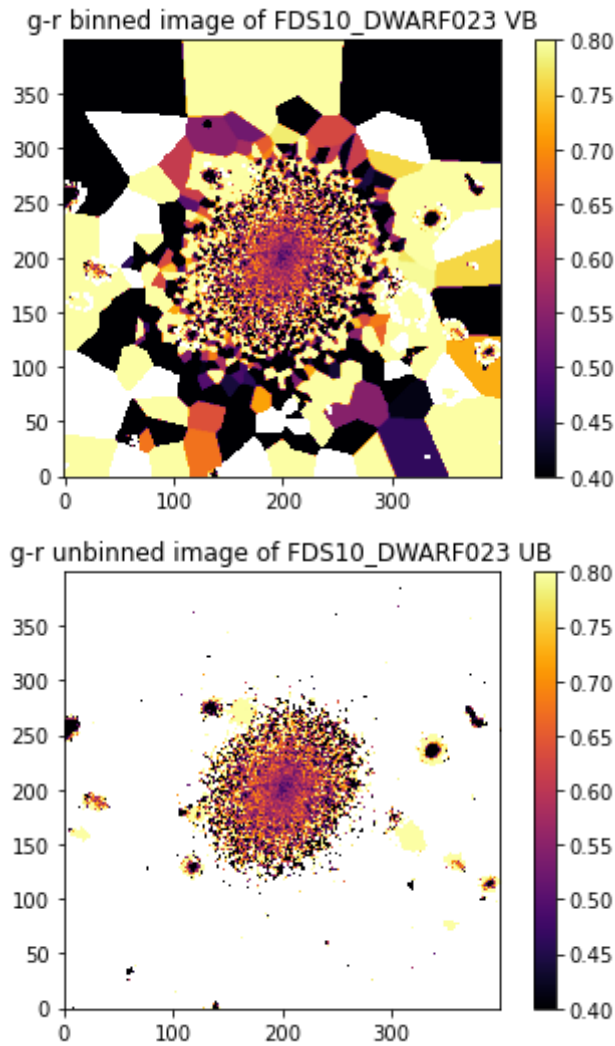


Figure 7.5: (top) the Voronoi binned g-r plot of FDS10\_DWARF023. (bottom) the unbinned version.

### FDS10\_DWARF189

The second dwarf galaxy investigated was FDS10\_DWARF189. With an effective radius of approximately 16 arcseconds and the lowest g- and r-band magnitudes within 1 effective radius out of the tile 10 sample, this is the brightest and largest dwarf of which the colour profile was computed. FDS10\_DWARF189 was the first galaxy on which the elliptical profile creation function was applied. Figure 7.6 shows the sampled area as well as the difference between the unbinned and Voronoi binned g-r profile.

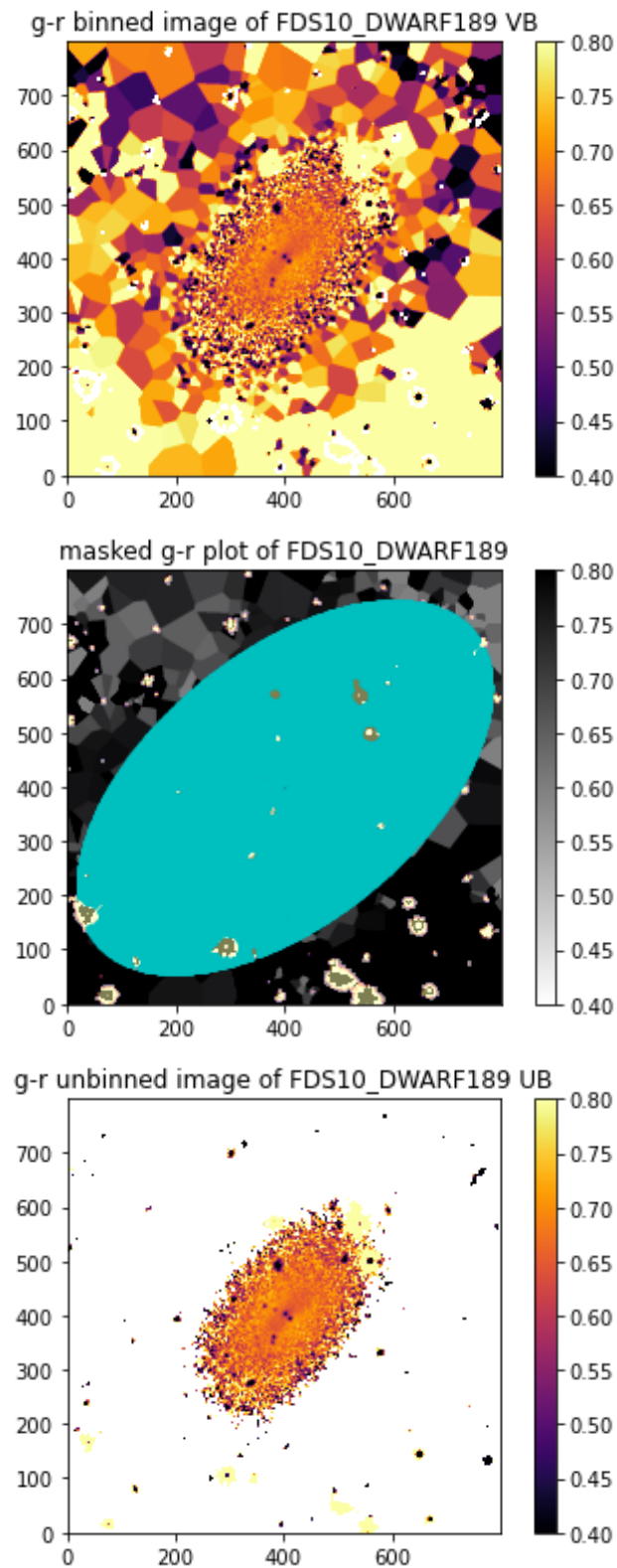


Figure 7.6: Top: the Voronoi binned g-r plot of FDS10\_DWARF189. Bottom: the unbinned version. In the middle: the area covered in the computation of the profile (turquoise), and the masked values (olive and cream). 1 effective radius corresponds to 80 pixels.

In figure 7.7, the g-r colour profile of FDS10\_DWARF189 is presented. Notice how, whilst the uncertainty does increase further away from the centre, one cannot observe the large blow up in uncertainty one can see in the profile of FDS10\_DWARF023. The profile does not extend far enough for the signal to be of the order of the noise. This is because a cropped (twice as small) version of the cut-out of FDS10\_DWARF189 was used to compute the profile, as the Voronoi binning process is very time consuming for large images. It was chosen to focus on different, smaller galaxies, instead of performing the process for the extended FDS10\_DWARF189 dataset.

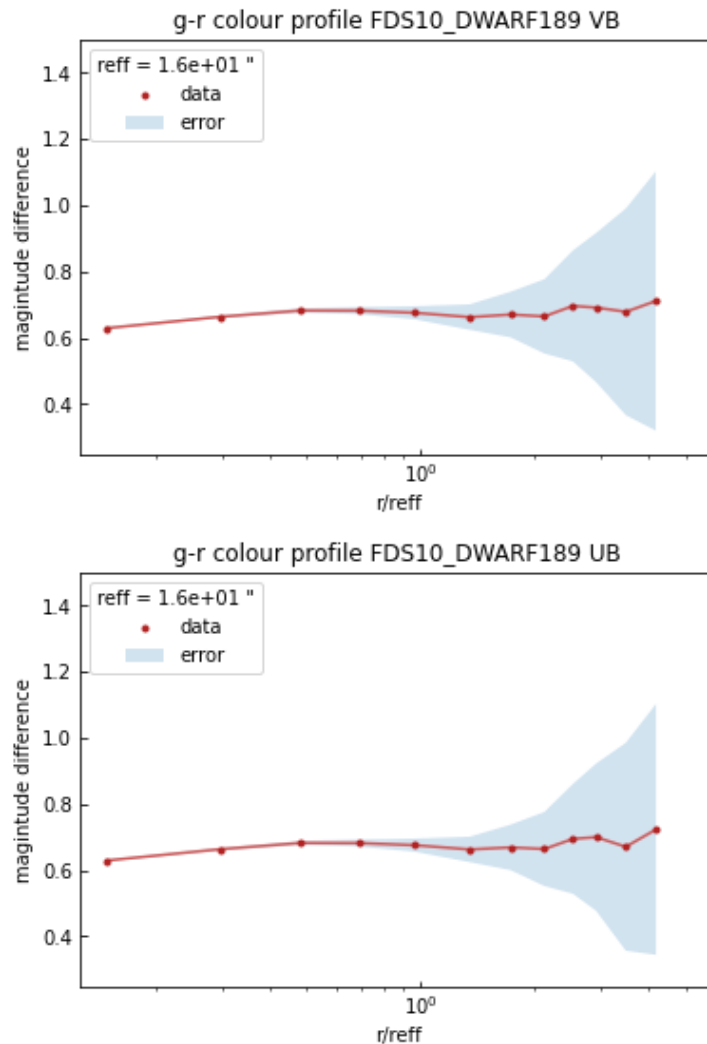


Figure 7.7: g-r profile of FDS10\_DWARF189 Voronoi binned (top), unbinned (bottom)

Both the Voronoi binned and the unbinned version of the profile are in agreement with each other until the last 0.5 effective radii, where both profiles show the same dip, yet the unbinned version has a steeper rise and fall in comparison with the Voronoi binned version. Reducing the ‘bumpiness’ in the profile is one of the effects of Voronoi binning one could expect to observe, as more binning reduces the impact of outliers and minor fluctuations.

Within 1 effective radius, the mean g-r value of both versions is 0.666 with an uncertainty of 0.02. The large uncertainty is because the presence of the source itself made it difficult to sample the background within the cropped image. The value obtained using the catalogue is 0.661 with an uncertainty of 0.05. Once again both values agree with each other within the margin of error.



### FDS10\_DWARF034

The faintest dwarf in the sample was FDS10\_DWARF034. Below, the pixel selection for the profile, as well as the g-r plots for this galaxy are presented. As shown in appendix C, the magnitude of the signal rises to values fainter than 31 magnitudes per square arcsecond after a distance of only 2 effective radii, approaching similar magnitudes as the estimated uncertainty in the background.

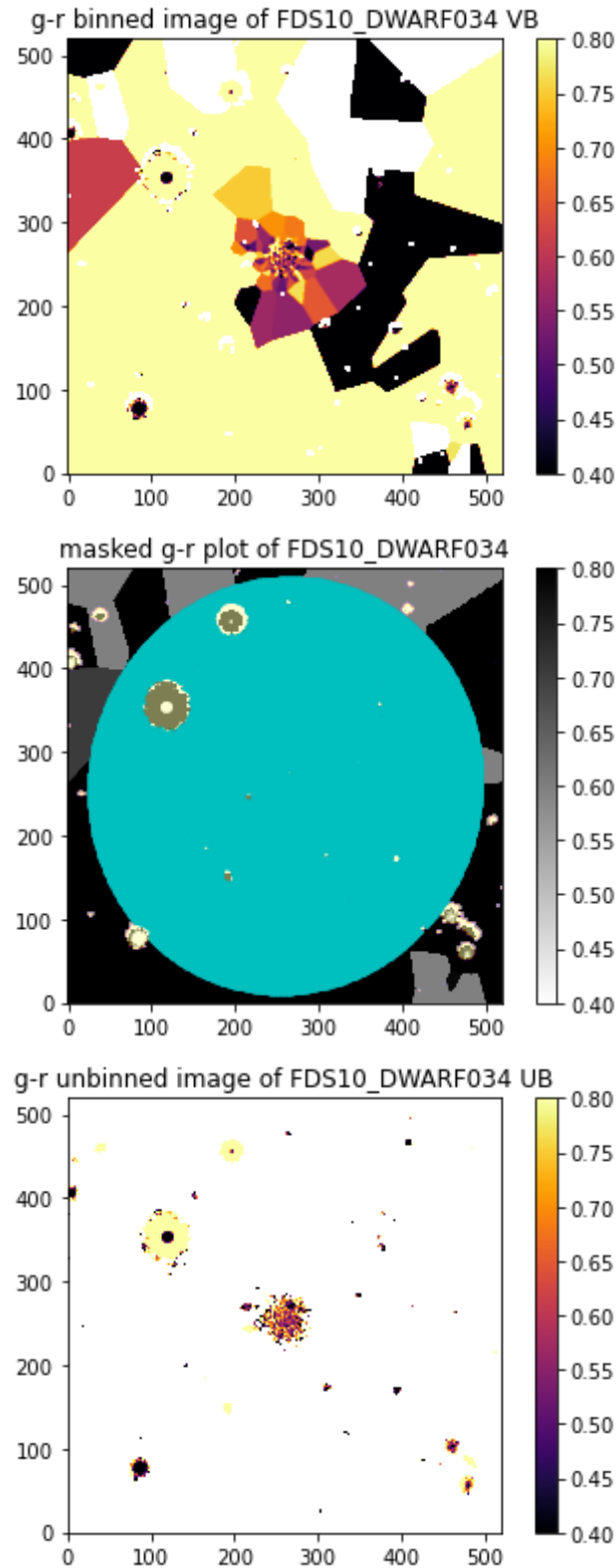


Figure 7.8: Top: the Voronoi binned g-r plot of FDS10\_DWARF034. Bottom: the unbinned version. In the middle: the area covered in the computation of the profile (turquoise), and the masked values (olive and cream). 1 effective radius corresponds to 26 pixels.

Figure 7.9 shows the resulting g-r profiles. There is a clear difference between the unbinned and Voronoi binned version, in the region where the uncertainty has already increased to values too large to be able to conclude something about the profile values with much certainty. Where the unbinned version shows a small rise, a fall and another rise, the Voronoi binned version shows a gradual increase.

Within the distance where the uncertainty is still small, one can see that as expected both profiles start out the same, after which, one can notice that the Voronoi profile is slightly straighter up to slightly over 1 effective radius.

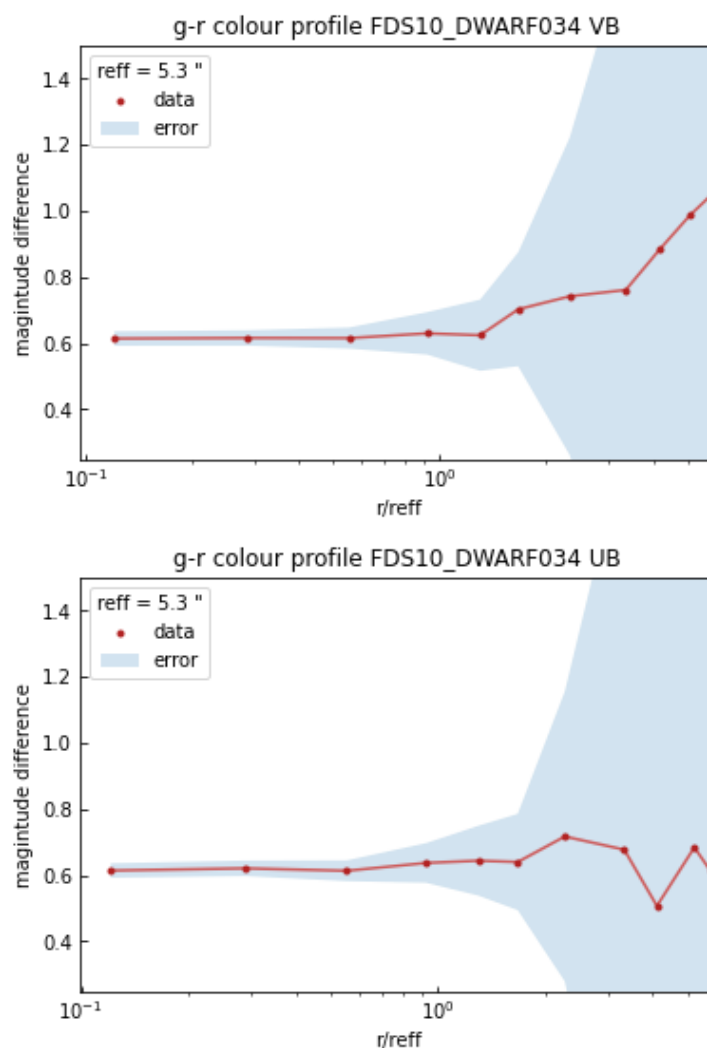


Figure 7.9: g-r profile of FDS10\_DWARF034 Voronoi binned (top), unbinned (bottom)

Within 1 effective radius, the mean value of g-r in the Voronoi binned version was found to be  $0.620 \pm 0.05$  and the mean value in the unbinned version  $0.626 \pm 0.05$ . The g-r value within 1 effective radius obtained using catalogue values was 0.640, also with an uncertainty of 0.05. All three values are in agreement with each other within their error margins.

### FDS10\_DWARF359

Below, the colour profile of FDS10\_DWARF359 is presented. Figure 7.10 shows the pixels taken into consideration as well as the difference between the Voronoi and unbinned g-r plot.

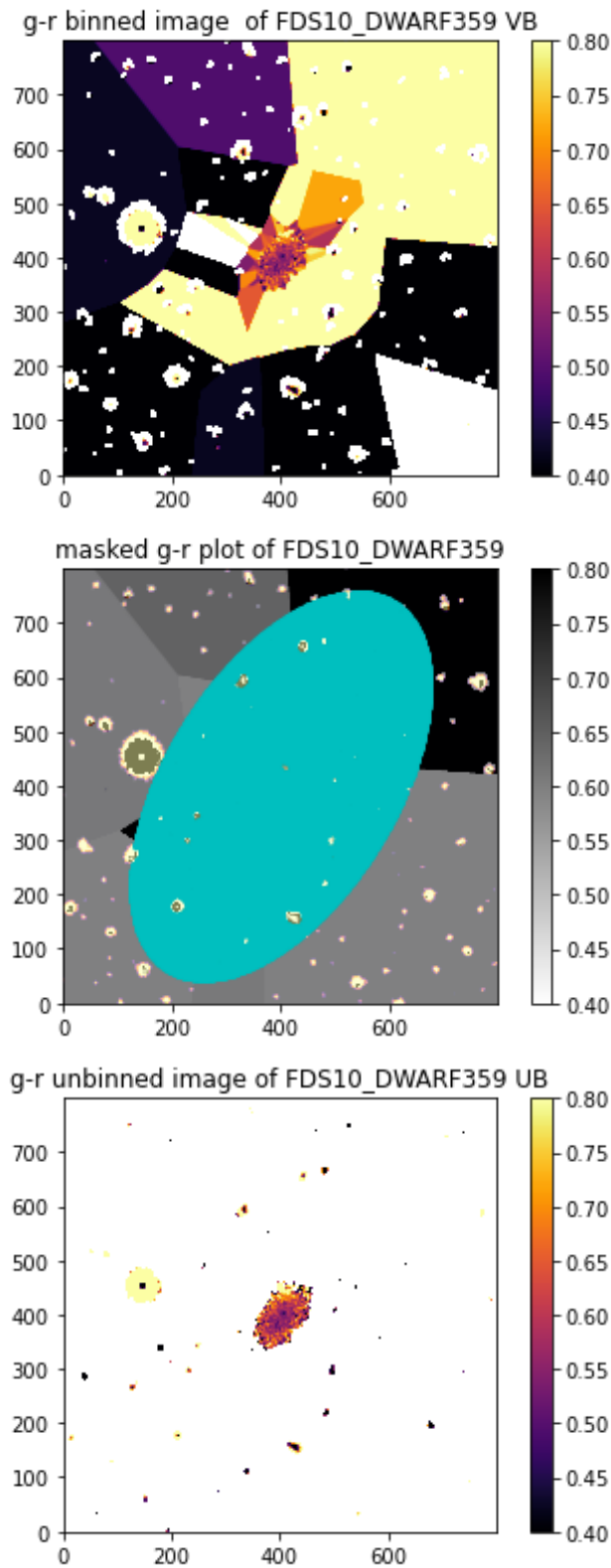


Figure 7.10: Top: the Voronoi binned g-r plot of FDS10\_DWARF359. Bottom: the unbinned version. In the middle: the area covered in the computation of the profile (turquoise), and the masked values (olive and cream). 1 effective radius corresponds to 40 pixels.

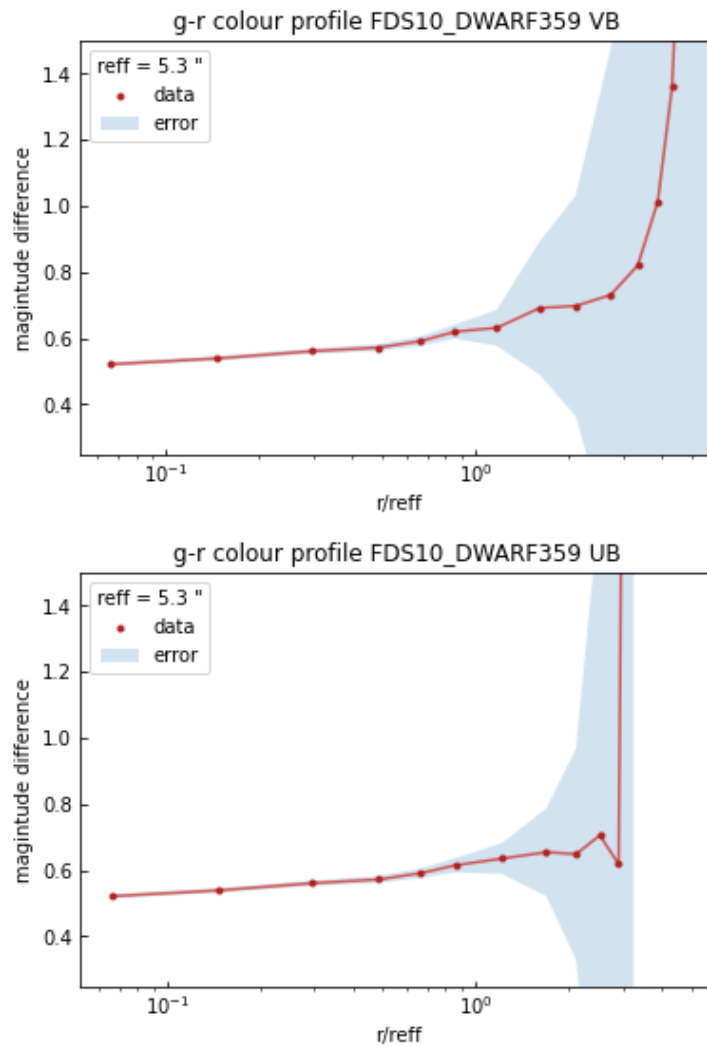


Figure 7.11: *g-r* profile of FDS10\_DWARF359 Voronoi binned (Top), unbinned (Bottom)

As can be seen in figure 7.11, both the Voronoi binned and the unbinned version of the profile begin similarly. The unbinned version has a minor peak and then a sudden rise around 3 effective radii, after which values are reached that result in a (non-existing) negative log when formula 4.1 is applied. The Voronoi binned version rises more gradually and continues to have existing values up to a larger distance than the unbinned version. The error has, however, blown up at a shorter distance, indicating that similar to the results for FDS10\_DWARF034 no conclusion can be drawn with much certainty.

Within 1 effective radius, the *g-r* colour of FDS10\_DWARF359 was found to be 0.576 in both the Voronoi binned and the unbinned version. The uncertainty was 0.02 in both cases. Using the catalogue values, one obtains  $0.579 \pm 0.05$ . Both values agree within their error margins, yet similar to FDS10\_DWARF023 and FDS10\_DWARF189, the values obtained in this research have a smaller uncertainty than the catalogue values.

To sum up, all the results for the colour within 1 effective radius have been found to be in agreement with the values obtained from the Venhola (2018) catalogue. The results regarding the advantage Voronoi binning might bring for determining the colour profile are, however, not very explicit. As expected, no clear difference between Voronoi binning and not Voronoi binning is observed at short

## The use of Voronoi binning in obtaining Colour profiles of FDS dwarfs

distances from the centre, where little to no pixels have been Voronoi binned. At greater distances, differences between the methods are observed. In general, the Voronoi binned profile shows more gradual transitions, it is less 'bumpy', compared to the unbinned version.

### Discussion

There are several factors one should bear in mind when considering the results presented in the previous chapters, as the choices made during the process impact the outcome and the scope of the project puts constraints to the detail up to which, for example, the various sources of noise in the background could have been taken into account.

#### Background reduction

The background reduction is perhaps the most crucial and difficult part of this project, as improper reduction leads to unreliable data, yet a large variety of irregular sorts of noise makes the reduction process tricky and time consuming. As explained in chapter 2, several measures have been taken to minimize the impact of the noise, yet there are several cases which may require a more complex form of background reduction than the one applied here. Although it does omit the central source and has some measures to avoid the impact of background sources, the linear background correction method does not correct for uneven gradients in the background, nor does it filter out any objects in the galaxies vicinity.

When creating a surface brightness profile of the data, it sometimes became apparent that the background was still slightly over- or under-subtracted. In the under-subtracted case, the profile flattens at a certain magnitude and in the over-subtracted case, the values become negative at larger distances instead of fluctuating around zero. If any of these two phenomena occurred, the subtracted constant was manually changed to a value where these phenomena do not occur. The manual value was picked to be such that within the estimated uncertainty in the background, the outermost few values of the profile approach zero. This problem only became apparent in the final stages of the project and there may be a different solution to the one mentioned above that may produce more reliable results, but due to time constraints this is something to investigate in another project. Further improvements can be made by for example extending the application of masks to all the dwarfs and by upgrading the grid-based background reduction function such that it automatically omits any sources in the background.

#### RGB creation

As shown in the results, one can, by properly reducing the background, picking the right scale function and, carefully adjusting the limits, create RGB images in which even high magnitude dwarf galaxies are clearly visible. With an exception of the smallest and faintest samples, the morphology of the galaxy, e.g. elliptical or irregular, was also clearly visible. Preserving the colours in a way that appeared natural, however, turned out to be challenging, as scaling the data interferes with the ratio between the bands. Determining exactly how a galaxy should appear and investigating whether there exists a way to provide all object with a 'realistic' colour goes, however, behind the scope of this project.

The initial tests on creating RGB's were done using the relatively bright and well-studied FDS11\_DWARF519, yet in the rest of the process, the main focus lay on the automatization of the RGB-creation. The downside to this approach is that, unless one works with many sub regimes, outliers in the data, e.g. very faint dwarfs with a nearby bright source or regions with non-linear backgrounds, will not yield a useful RGB-image. In addition, as shown by the histograms, the u- and i-band shape deviated greatly from that of the r- and g- band. To combat this, these band were scaled, yet the difference in signal strength and noise remained apparent. Most of the ugr-images appear somewhat yellow, with minor blue freckles in the background. Re-adjusting the limits caused an even bluer background or an entirely yellow source, thus a different approach is needed to handle the u-band. In the gri-images, this problem does not occur this strong, yet some of the sources display a

slightly red or green freckled background, as can be seen in Appendix B. As the background related problems differ per image and some images seem to have the desired black background, it is shown that sometimes an individual approach is needed.

### Colour profiles

Apart from the previously discussed background related points, there are a few additional remarks to be made about the colour profiles. Several assumptions were made in this research concerning the results presented in chapter 7. For example the chosen value of 100 when determining the Voronoi bins and the sizes of the ring shaped bins in the profiles. In the previous chapters, the motivation behind the choices made is explained, yet bear in mind that the results might be different under another set of assumptions.

Similarly to the process of determining the constant that needed to be subtracted from the background, the process of determining the uncertainty in the background depends on the areas where one samples the values. In this case several boxes were sampled in regions that appeared to be empty and far away from the source. There may be more reliable methods to select sampling regions that increase the reliability of this estimate, for example setting certain numerical criteria for selecting the regions rather than picking a couple of areas that appear to be empty by eye.

On a different note, an interesting find is that all the computed g-r colour profiles are either flat or have a small positive colour gradient. Su et al. (2021) has also investigated the gradient in g-r colour of dwarfs in the Fornax cluster by determining the difference the colour within 0.5 effective radii and the colour in the 1-2 effective radii region. There, it was found that the average colour difference is approximately zero and that where the most massive galaxies tend to have negative colour differences, the less massive galaxies can have positive as well as negative gradients. The galaxies studied in chapter 7 fall into the mass range where one would indeed expect the colour gradient to be approximately zero or positive based on these findings.

### General Remarks

Before commencing this project, the author did not have any experience on working with FDS data or creating colour profiles. To make use of the author's experience with Python in the process of developing understanding and intuition regarding the research matter, it was chosen to create the data pipeline from the tile data to the profiles manually, using several python packages as basis. The benefit of this approach is that it is easy to finetune to the specific needs of the project and that the code is very accessible to adjust or debug. The downside is that the resulting code is relatively primitive and it is, thus, also assumable that there are many ways in which the pipeline can be optimised. In addition it turned out to be quite time consuming to debug the function for creating the colour profile with errors. In a future project the author will reserve more time for possible debugging in the initial schedule. Lastly, some elements of the current code take a long time to run. The complexity of several functions can likely be decreased by looping differently or combining steps, which would make the code significantly faster.

All in all, when examining the results of this research one should bear in mind the impact of the assumptions made and the limitations of the methods applied. In a future project one can use the scripts developed in this research along with the recommendations posed to improve the current results and obtain a higher accuracy and precision.



## Conclusion

During this project rgb-images and colour profiles of several dwarf galaxies have been computed. To achieve this, several scripts have been developed:

- An automated script to crop one large dataset into smaller ones of a specified relative size centred around given coordinates.
- Methods to linearly correct the background or to rescale it based on its histogram (do keep in mind that the latter should only be used to enhance images meant to be aesthetic)
- A spherical and elliptical ring-based binning function that uses a given array of outer radii, which can be used to create galactic profiles.

In addition, research has been done to understand and apply the pre-existing Voronoi binning algorithm and pre-fabricated masks on the FDS and to access ds9 from a python environment. All of this resulted into several series of rgb-images of 52 different dwarf galaxies, both Voronoi- and not Voronoi-binned colour profiles of 4 dwarf galaxies and countless useful insights into the process of conducting scientific research. At the start of this report, three project objectives were defined. Below, the conclusion and the points of discussion per goal are summed up and critically examined.

### 1. *Does Voronoi binning improve the colour profile at low surface brightness?*

The main question examined in this project is whether applying Voronoi binning will enable one to determine the colour profile of dwarf galaxies within a certain accuracy up to lower levels of surface brightness compared to not binning the data. This turned out to be quite difficult to determine as the accuracy in the removal of the background gravely impacts the resulting profile, which led to no satisfactory answer to the research question other than that the trend appears to be that the Voronoi binned profiles tend to be less 'bumpy' and the profiles extend a little further before turning to impossible value, yet this is only after the uncertainty has already increased to very large sizes. Voronoi binning locally increases the signal to noise ratio, but it does not affect systematic problems in the sky determination.

As shown in the discussion section, several measures have been taken to correct the background but there are still many more ways in which this can be improved.

In addition, there are many parameters involved during both the binning and the profile making process. Although a justification is provided for the choice of parameters in this research, choosing a different noise or target signal to noise in the binning process or input list of radii and linear background correction constant might lead to interesting or better results.

Finally, the final size of the sample for the profiles, 4 different dwarfs, is smaller than initially hoped for. In a follow-up research one could extend this sample with a larger subset of dwarfs and investigate them to a larger detail. One could examine a larger sample of the FDS dwarfs or investigate similar data from a different survey and compare the results.

Most of these suggestions were not implemented in this research due to time constraints. It took quite some time to get acquainted with the data, programs (SAODS9, Aladin) and python packages (AstroPy, VorBin) and to gain the knowledge needed on the front of astronomical image processing to be able to examine the main research question. In a longer research project or one conducted by someone with more experience in this field, one will be able to examine the question in further detail. It can, however, be concluded that the results acquired in this research concerning the g-r colour of the profiles are reliable, as in each of the presented cases, the g-r colour within 1 effective radius is in agreement with the value obtained from the Venhola (2018) catalogue and has an uncertainty equal to or smaller than the catalogue value.

2. *Can one create realistic rgb-images from the FDS data?*

The second objective of this project is to create RGB pictures of dwarf galaxies from FDS data which look realistic and preserve their characteristics regarding colour and structure. By working with various regimes and carefully selecting the limits and scale function, a series of images was produced that appears in accordance with the expectations one might have for the colour of a galaxy and that indeed preserves the morphology of the galaxy (as was specified in the catalogue). Although the assignment of bands to colours was done using preserving the underlying science, the rescaling of the bands does disrupt the relation between the bands and thus the scientific colour. In future research, one can investigate a way to preserve this colour better. The current final series of images can, however, be used for outreach purposes when it comes to promoting the FDS and the research done with it. Images are of great importance to provide a non-expert audience with an idea of the research you are conducting and speak more to the imagination of your audience than raw or numerical data.

3. *What does doing research entail?*

This third objective is not related to the scientific conclusions drawn but rather related to the author's personal development. In the master of Science Communication, the Scientific Research Project is aimed to give students insight into what it actually means to do research, which will be useful knowledge when writing about the research of others. Although it is not possible to objectively verify up to what extent this objective has been reached, in the author's opinion this project has succeeded into showing her what doing research entails. Before this project, the author's experience in doing research consisted of the research projects during the Astronomy bachelor, which were either at most a few weeks in length or oriented at outreach, rather than conducting science. In this project the author learned that conducting research is a far more gradual process than the stepwise 'background research -> method -> results' it appears to be at first glance. Whilst conducting research, one also develops one's own understanding of the topic, which can change the way one looks at the subject or the approach one wants to take.

In addition to doing and discussing her own research project, the author got to join the bi-weekly meetings of the SUNDIAL research group, in which each meeting another astronomical paper is discussed, after which a guest speaker provides some extra insights or several group members tell something about the progress they have made with their own research. Through these informal meetings, one gains more insight into recent developments in the field of astronomical research and the views of experts on these topics. In addition one can gain expert feedback on one's own project and practise presenting it, which makes the meetings useful regarding both one's own research and one's general knowledge of the field. Before starting this project, the author had not expected research included meetings like this, yet it seems a valuable addition.

All in all one can thus conclude that

- The methods developed in this chapter are suitable for determining the colour of galaxies.
- Voronoi binning appears to result in less 'bumpy' colour profiles, yet whether it is an improvement compared to the unbinned version requires further investigation.
- A set of RGB images with nice applications for outreach have been created.
- The author's understanding of both the subject matter and the meaning of conducting scientific research have improved.

Making this science research project successful in achieving its goals.

## Acknowledgements

The author would like to thank Shivangee Rathi for providing the masks and Reynier Peletier for the guidance throughout the project.

## References

The data was obtained from:

<http://www.astro.rug.nl/~fds/data.html> and is also available on <https://eso.org/sci/publications/announcements/sciann17326.html>  
Information on the VST/OmegaCam: <https://www.eso.org/public/teles-instr/paranal-observatory/surveytelescopes/vst/camera/>

Coordinates, effective radii and values for comparison were obtained from:

*Fornax Deep Survey with VST. IV. Dwarf galaxies* (Venhola et al., 2018) catalogue: <https://vizier.u-strasbg.fr/viz-bin/VizieR-3?-source=J/A%2bA/620/A165&-out.max=50&-out.form=HTML%20Table&-out.add=r&-out.add=RAJ,DEJ&-sort=r&-oc.form=sexa>

In addition some values were obtained from the NASA/IPAC Extragalactic Database:

[http://ned.ipac.caltech.edu/byname?objname=NGC1427A&hconst=67.8&omegam=0.308&omegav=0.692&wmap=4&corr\\_z=1](http://ned.ipac.caltech.edu/byname?objname=NGC1427A&hconst=67.8&omegam=0.308&omegav=0.692&wmap=4&corr_z=1)

The following are references for the programs and Python packages used:

AstroPy: <https://www.astropy.org/>

Funpack: <https://heasarc.gsfc.nasa.gov/fitsio/fpack/>

SAODS9: <https://sites.google.com/cfa.harvard.edu/saomageds9/home>

VorBin: <https://pypi.org/project/vorbin/>

Papers and other sources used/referenced:

Arnaboldi et al. 1998 (Arnaboldi, M., Capaccioli, M., Mancini, D., Rafanelli, P., Scaranella, R., Sedmak, G. and Vettolani, G. P., 1998. *The Messenger* 93, 30)

Aurenhammer et al. (1999) "Chapter 5 - Voronoi Diagrams", *Handbook of Computational Geometry*, 201-290, ISBN 9780444825377, <https://doi.org/10.1016/B978-044482537-7/50006-1>

Blanton et al. (2005) "Relationship between Environment and the Broadband Optical Properties of Galaxies in the Sloan Digital Sky Survey" *The Astrophysical Journal* **629** L143-L157 doi: 10.1086/422897

Cappellari, Copin (2003) "Adaptive spatial binning of integral-field spectroscopic data using Voronoi tessellations", *Monthly Notices of the Royal Astronomical Society*, Volume 342, Issue 2, 345–354, <https://doi.org/10.1046/j.1365-8711.2003.06541.x>

Diehl, Statler (2006) "Adaptive binning of X-ray data with weighted Voronoi tessellations", *Monthly Notices of the Royal Astronomical Society*, Volume 368, Issue 2, 497-510, <http://dx.doi.org/10.1111/j.1365-2966.2006.10125.x>

Drinkwater, et al.(2001) "Substructure and Dynamics of the Fornax Cluster." *The Astrophysical Journal* **548**, L139–L142. doi:10.1086/319113

ESA-Hubble, "A short introduction to astronomical image processing" [https://esahubble.org/projects/fits\\_liberator/improc/](https://esahubble.org/projects/fits_liberator/improc/)

Fukugita et al. (1996). The Sloan digital sky survey photometric system (No. IASSNS-AST-96-3). SCAN-9601313.

Haigh et al.(2021) "Optimising and comparing source-extraction tools using objective segmentation quality criteria." *Astronomy and Astrophysics* **645**. doi:10.1051/0004-6361/201936561

Kuijken et al. 2002 (*The Messenger*, 110, p. 15, 2002) and Kuijken 2011 (*The Messenger*, vol. 146, p. 8, 2011).

Lee-Waddell et al. (2018) "Tidal origin of NGC 1427A in the Fornax cluster." *Monthly Notices of the Royal Astronomical Society*, **474**, Issue 1, 1108–1115, <https://doi.org/10.1093/mnras/stx2808>

Mentz et al. (2016). Abundance ratios and IMF slopes in the dwarf elliptical galaxy NGC 1396 with MUSE. *Monthly Notices of the Royal Astronomical Society*, 463(3), 2819-2838.

## The use of Voronoi binning in obtaining Colour profiles of FDS dwarfs

Parikh et al. (2021). SDSS-IV MaNGA: radial gradients in stellar population properties of early-type and late-type galaxies. *Monthly Notices of the Royal Astronomical Society*, 502(4), 5508-5527.

Peletier et al.(1999) "Galactic bulges from Hubble Space Telescope NICMOS observations: ages and dust." *Monthly Notices of the Royal Astronomical Society* **310**, 703–716. doi:10.1046/j.1365-8711.1999.02980.x

Su et al. (2021) "The Fornax Deep Survey (FDS) with the VST. XI. The search for signs of pre-processing between the Fornax main cluster and Fornax A group." *Astronomy and Astrophysics* **647**. doi:10.1051/0004-6361/202039633

Taylor et al.(2011) "Galaxy And Mass Assembly (GAMA): stellar mass estimates." *Monthly Notices of the Royal Astronomical Society* **418**, 1587–1620. doi:10.1111/j.1365-2966.2011.19536.x

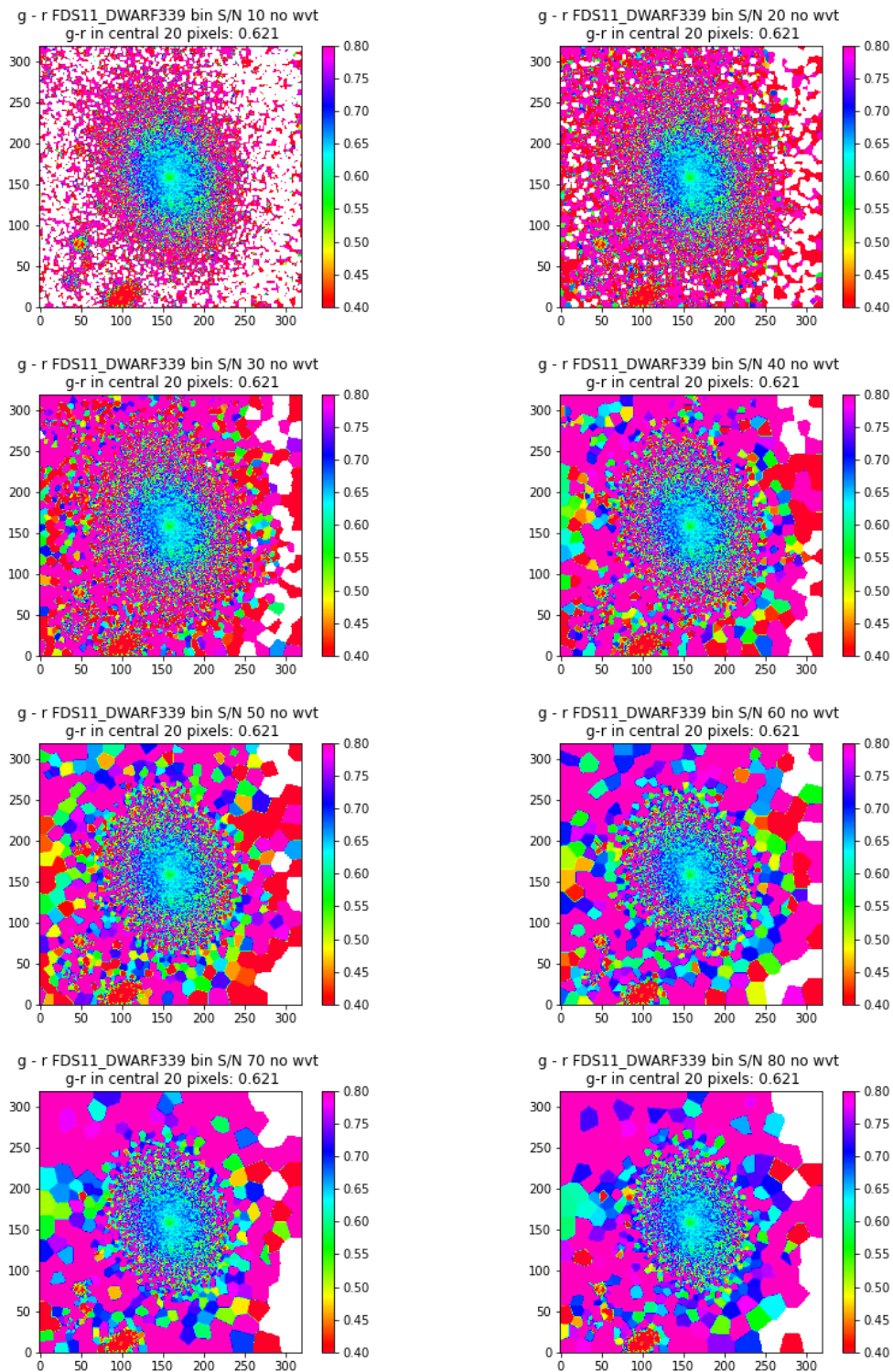
Venhola et al. (2018) "The Fornax Deep Survey with the VST. IV. A size and magnitude limited catalog of dwarf galaxies in the area of the Fornax cluster." *Astronomy and Astrophysics* **620**. doi:10.1051/0004-6361/201833933

Venhola et al. (2019) "The Fornax Deep Survey (FDS) with VST - VI. Optical properties of the dwarf galaxies in the Fornax cluster" *Astronomy and Astrophysics* **625** A143 doi: 10.1051/0004-6361/201935231

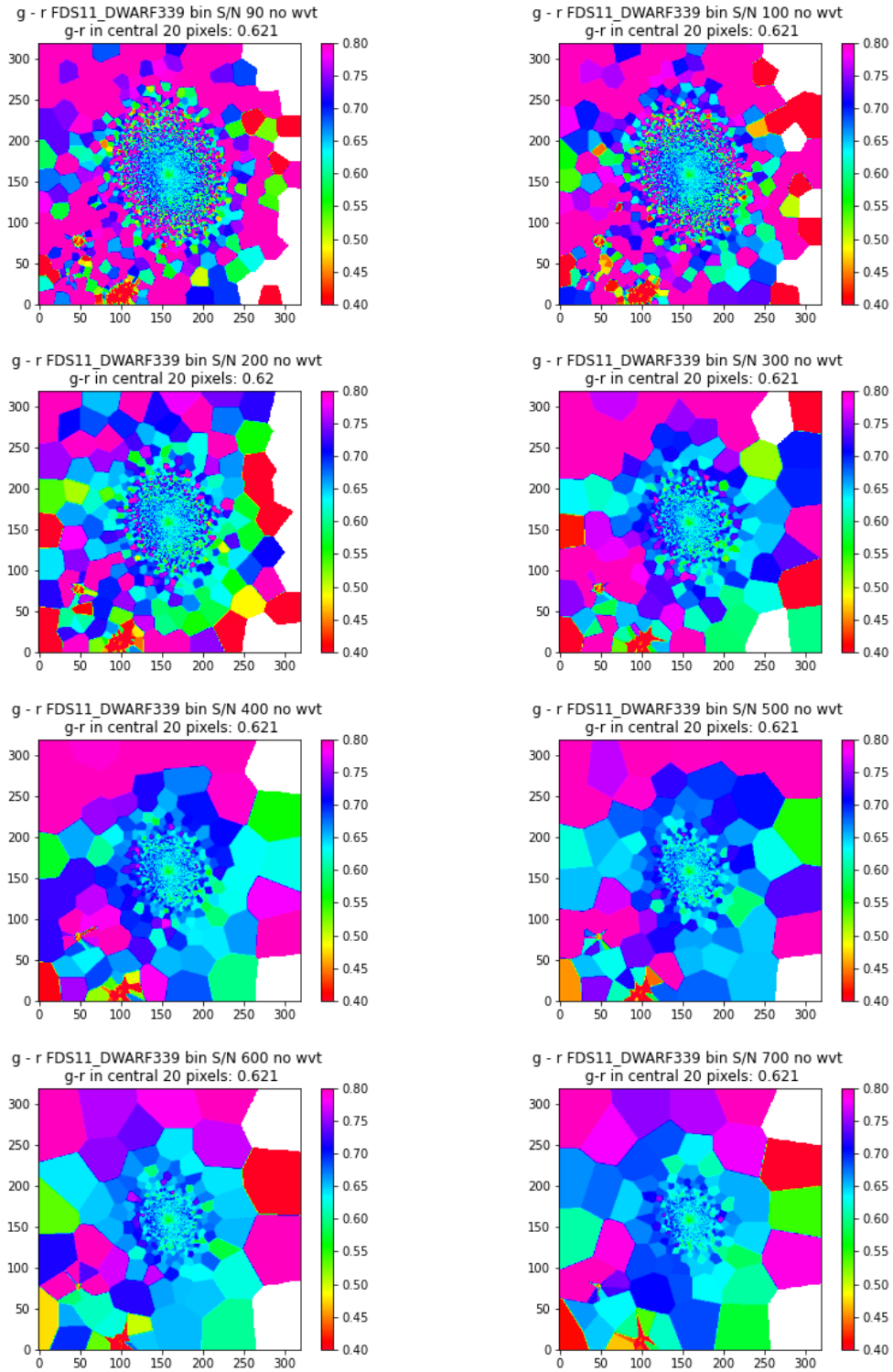
Weisstein, "Voronoi Diagram." MathWorld—A Wolfram Web Resource, <https://mathworld.wolfram.com/VoronoiDiagram.html>

## Appendix A: an overview of Voronoi binned g-r diagrams with varying target signal to noise

All diagrams were made using the same dataset and VorBin input. Only the target signal to noise was varied. The binning was done using a noise set to the standard deviation of the data divided by 100. The binning algorithm was set to only cvt. The diagrams range from a target signal to noise of 10 up until 9000.

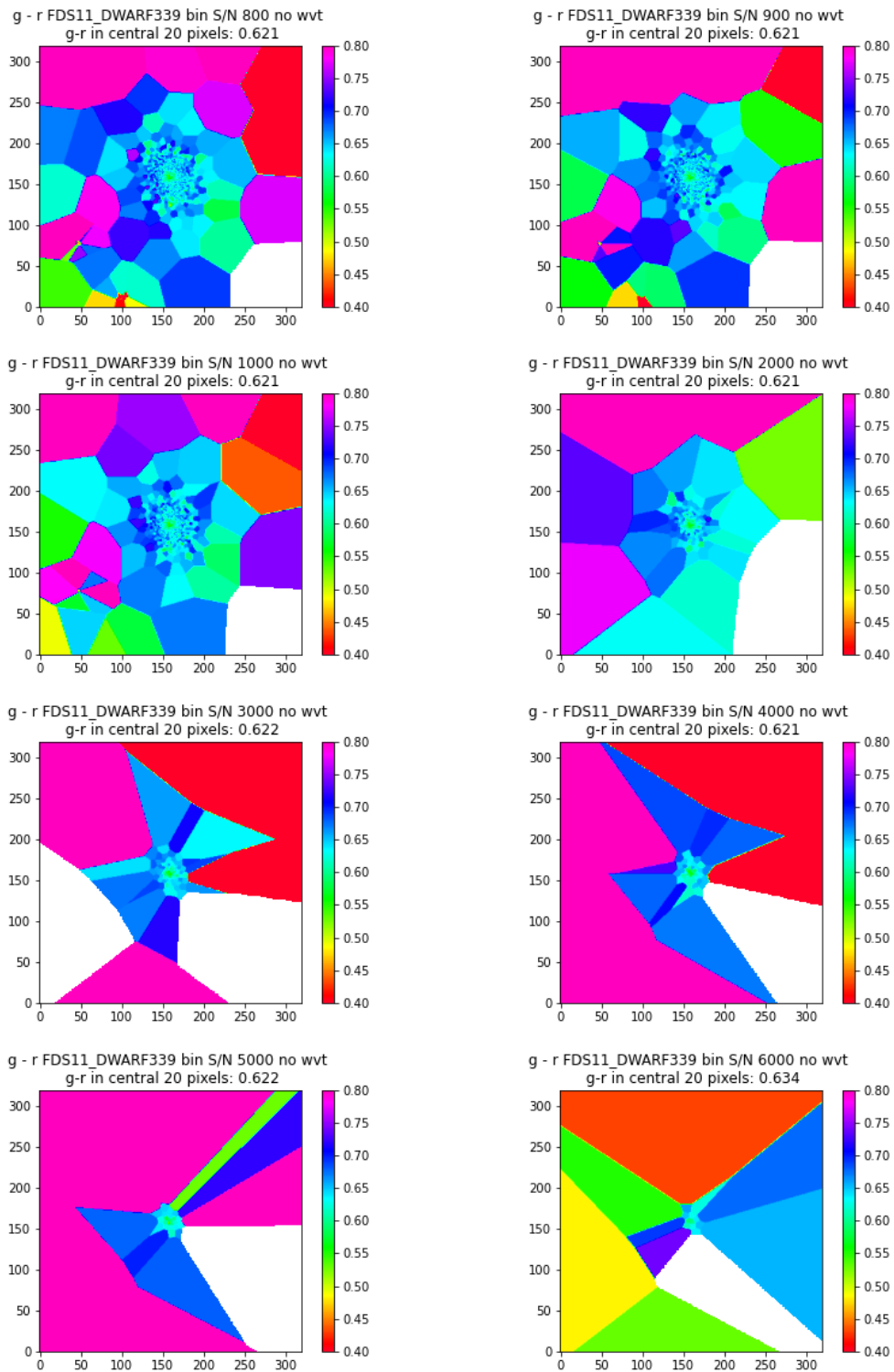


# The use of Voronoi binning in obtaining Colour profiles of FDS dwarfs

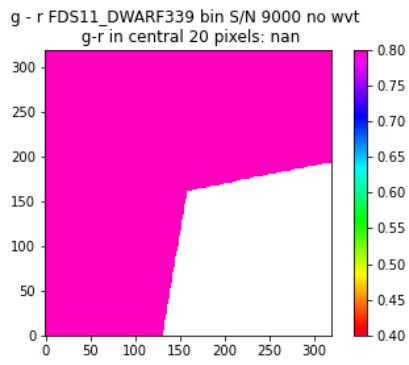
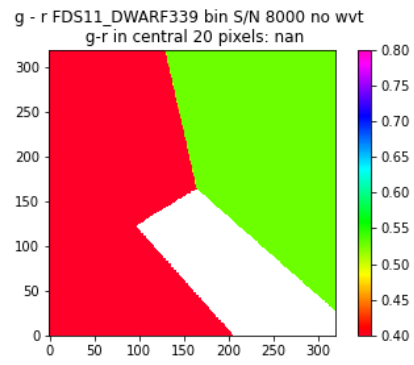
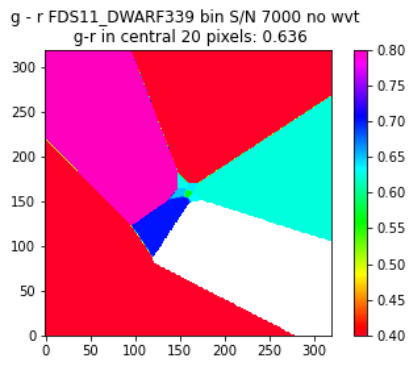




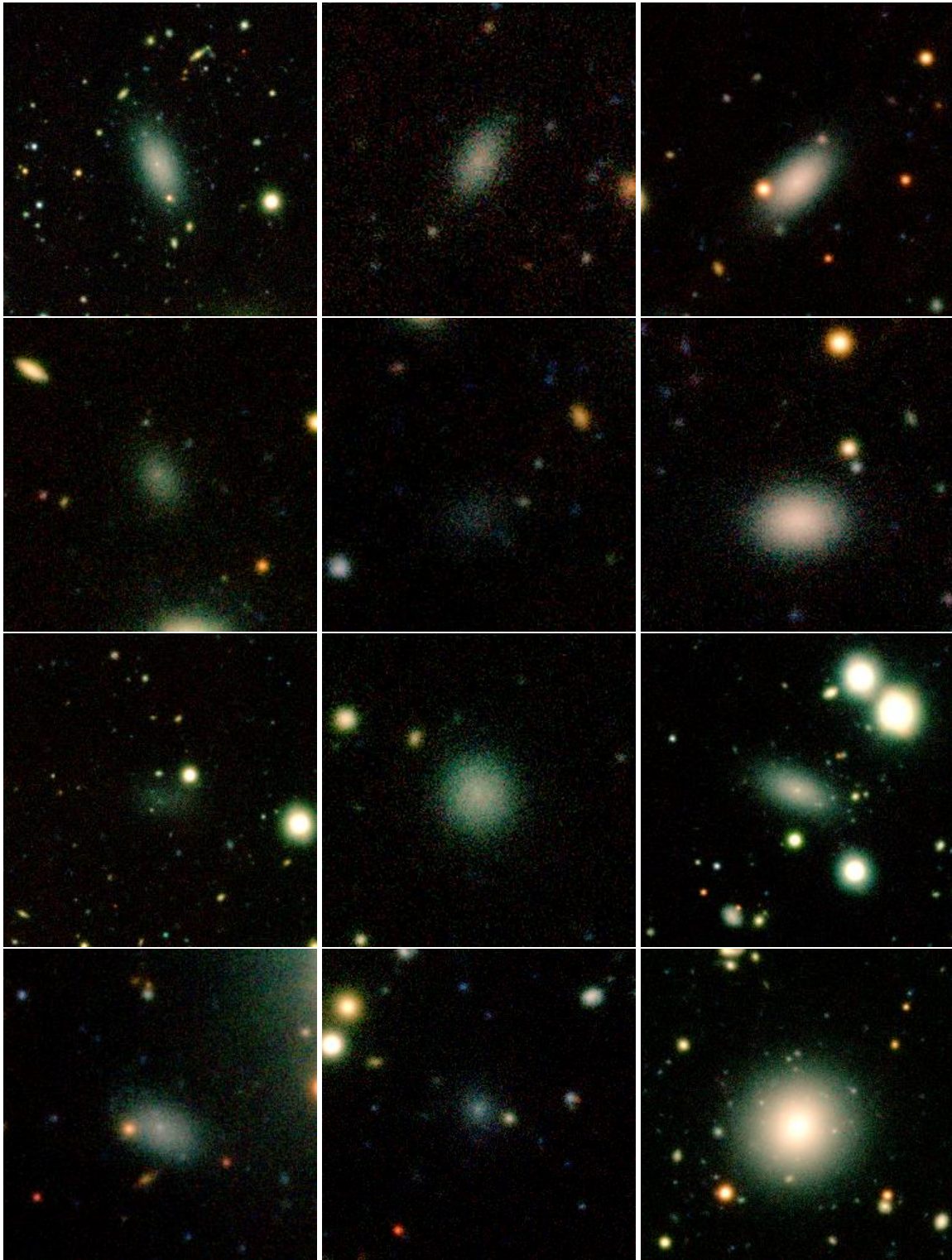
# The use of Voronoi binning in obtaining Colour profiles of FDS dwarfs



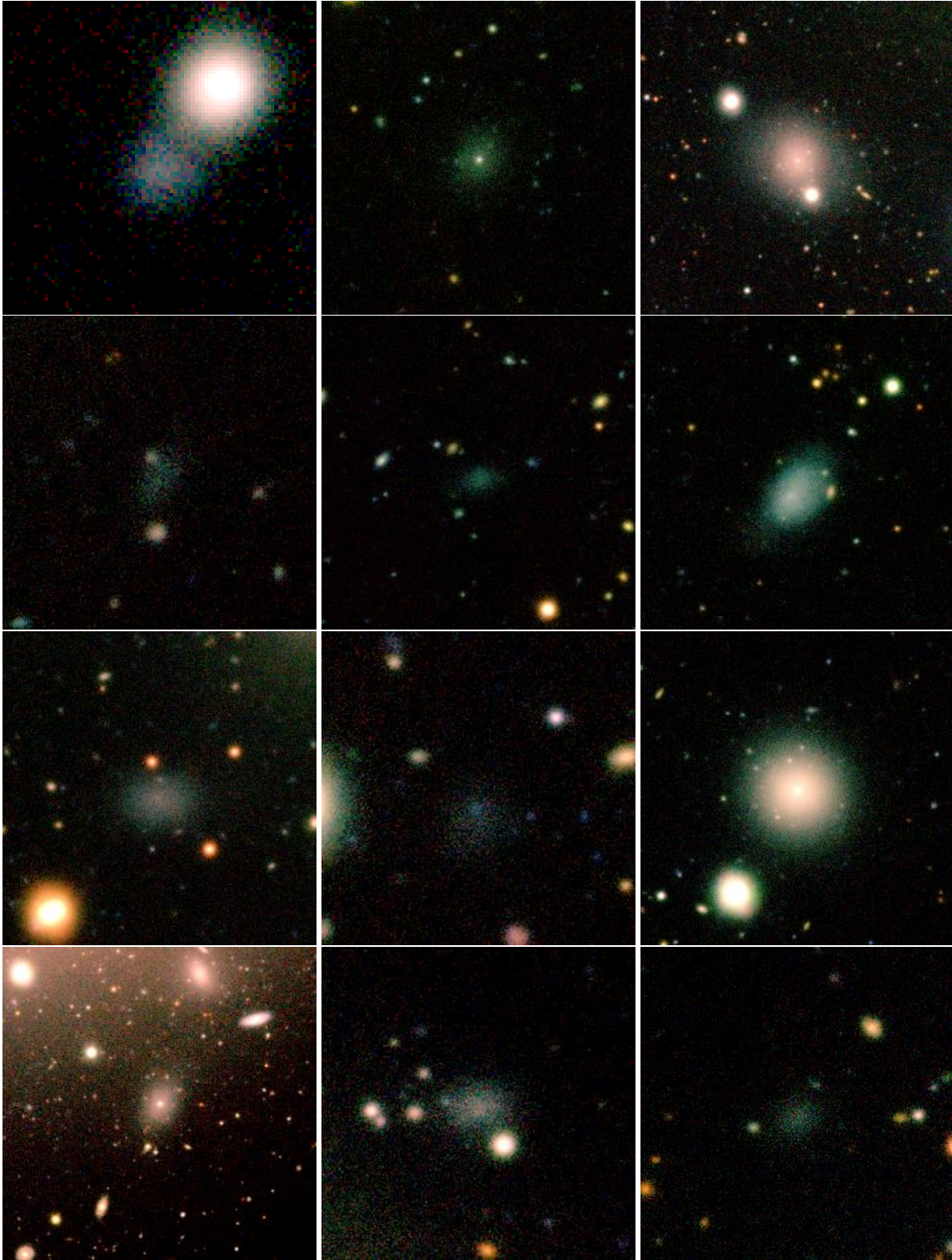
# The use of Voronoi binning in obtaining Colour profiles of FDS dwarfs



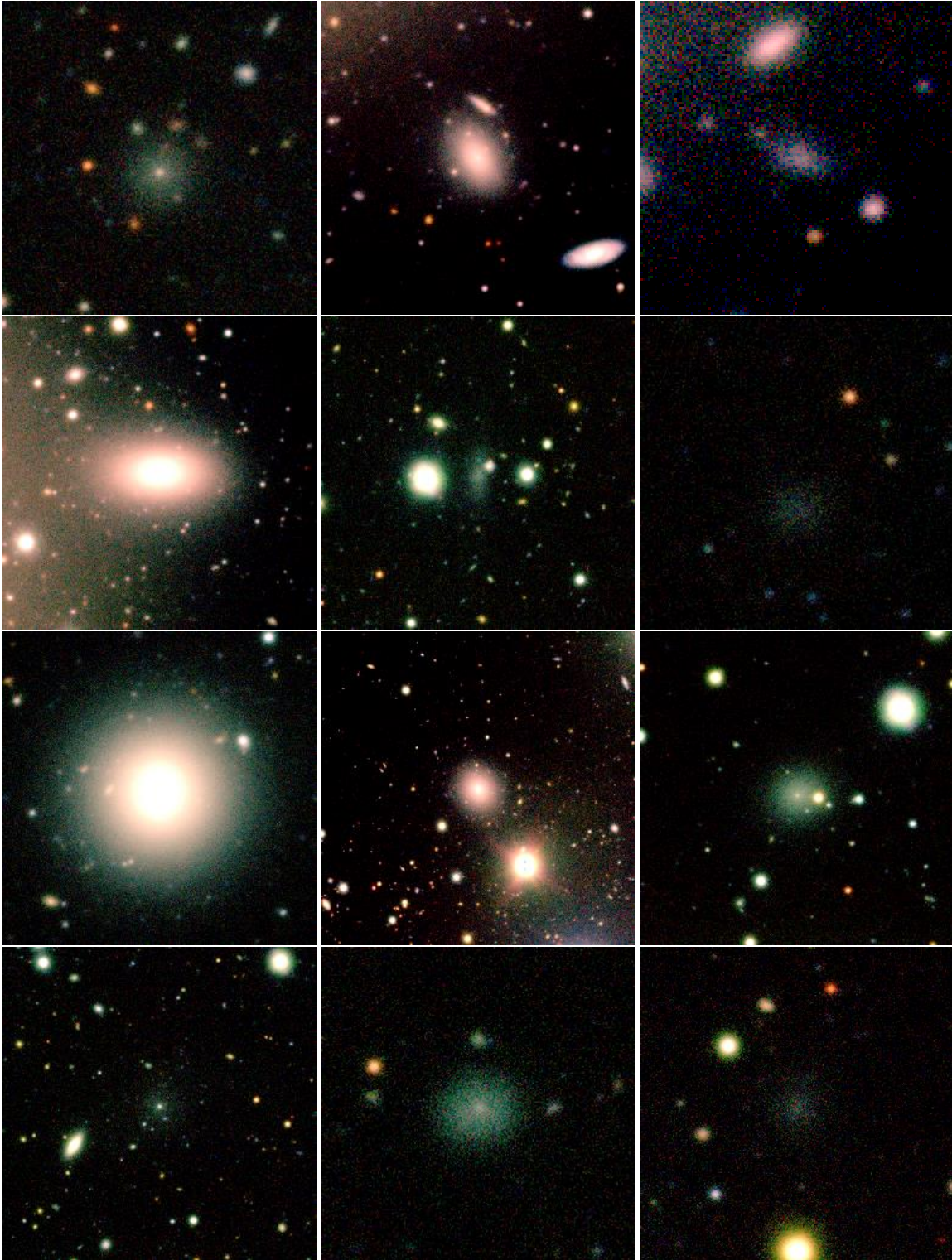
Appendix B: Tile 11 dwarf galaxy RGB-images of the g- (blue), r- (green) and i- (red) bands.



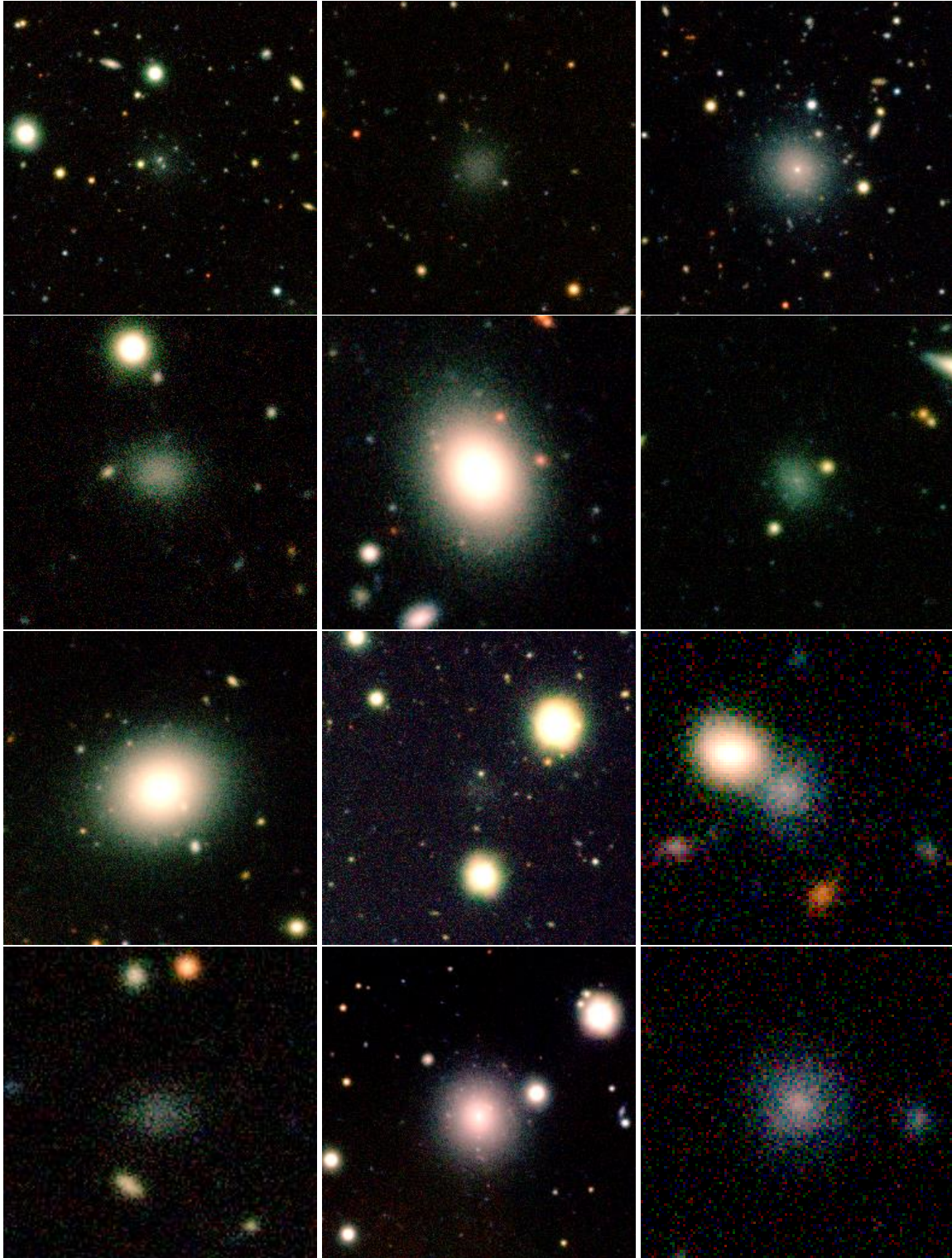


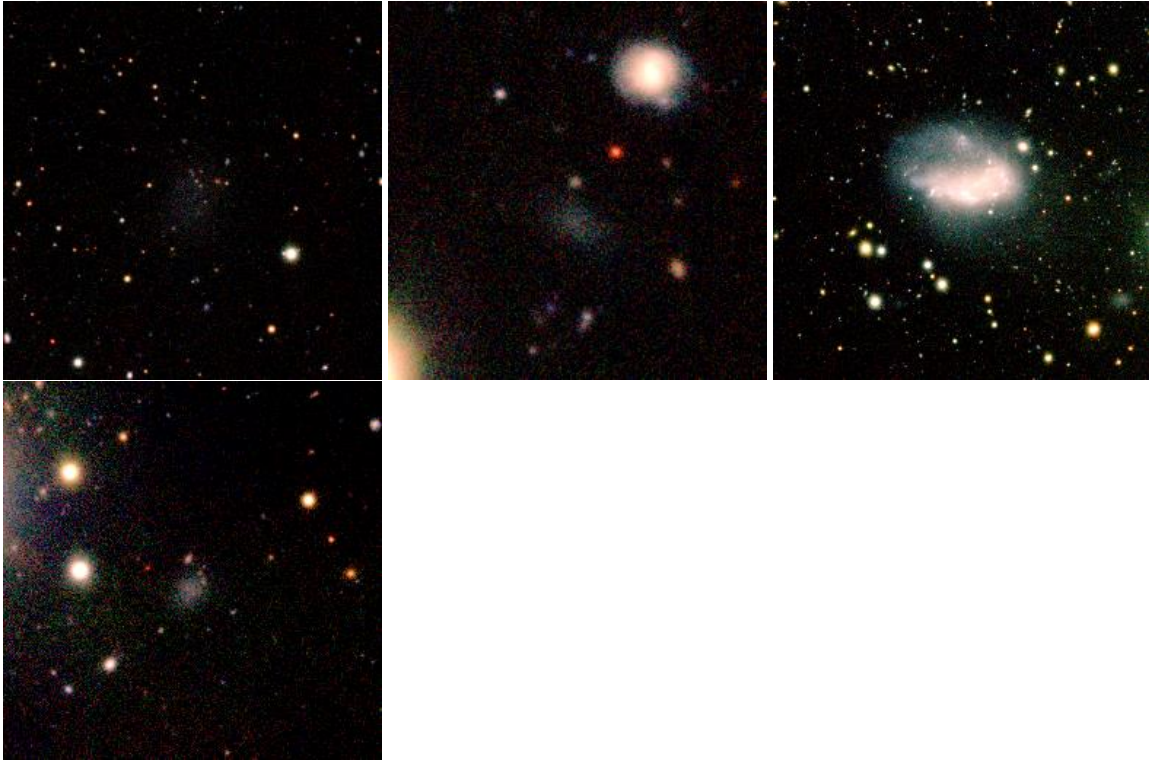














## Appendix C: Tables/factsheets

An overview of the catalogue values used in the calculations and the numerical output for the colour profile. VB stands for Voronoi binned data, UB is the data without Voronoi binning.

\*= values from the Venhola (2018) catalogue

### FDS10\_DWARF023

Sampled uncertainty in the background:

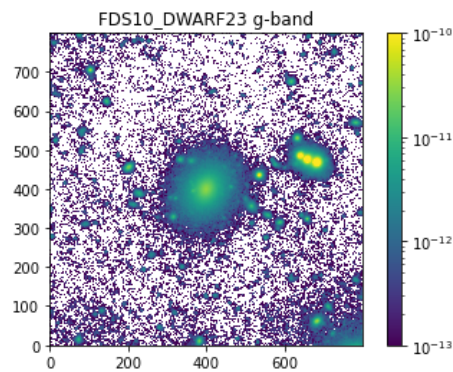
r-band uncertainty =  $7.6e-14$

g-band uncertainty =  $7.0e-14$

Stellar mass estimate\* =  $4.75e7 M_{\odot}$

Apparent r-band magnitude  $< 1 r_{\text{eff}}^* = 17.6905$

R.A. (deg)*	Decl. (deg)*	$R_{\text{eff}}^*$ (arcsec)	PA* (deg)	arat*	Alternative names*
054.4777	-34.8821	8.051080	-33.062599	0.814300	FCC200, LEDA 74802, NGFS033755-34525



Pixel radius = 40

Weighted $r/r_{\text{eff}}$		g-r		error g-r		g-band		error g-band		r-band		error r-band	
UB	VB	UB	VB	UB	VB	UB	VB	UB	VB	UB	VB	UB	VB
0.084	0.084	0.518	0.518	0.003	0.003	26.329	26.329	0.003	0.003	25.811	25.811	0.002	0.002
0.190	0.190	0.546	0.546	0.004	0.004	26.497	26.497	0.003	0.003	25.951	25.951	0.002	0.002
0.377	0.377	0.584	0.584	0.005	0.005	26.906	26.906	0.004	0.004	26.322	26.322	0.003	0.003
0.620	0.620	0.598	0.598	0.009	0.009	27.467	27.467	0.007	0.007	26.869	26.869	0.005	0.005
0.872	0.872	0.611	0.611	0.014	0.014	27.984	27.984	0.012	0.012	27.373	27.373	0.007	0.007
1.120	1.120	0.615	0.615	0.022	0.022	28.467	28.467	0.019	0.019	27.852	27.852	0.011	0.011
1.586	1.586	0.613	0.615	0.045	0.045	29.254	29.256	0.038	0.038	28.641	28.642	0.024	0.024
2.234	2.231	0.639	0.631	0.106	0.106	30.189	30.193	0.091	0.091	29.550	29.561	0.055	0.055
2.777	2.776	0.611	0.625	0.231	0.239	31.028	31.073	0.204	0.204	30.417	30.448	0.125	0.125
3.390	3.390	0.647	0.633	0.641	0.640	32.148	32.143	0.547	0.547	31.501	31.510	0.334	0.334
3.988	4.006	1.470	1.262	4.536	3.954	34.399	34.231	3.741	3.741	32.929	32.970	1.280	1.280

FDS10\_DWARF034

*This source is the faintest source in this sample.*

Sampled uncertainty in the background:

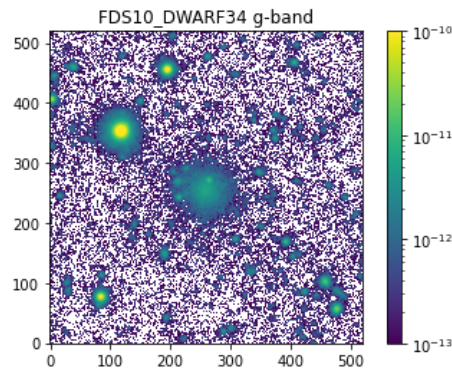
r-band uncertainty =  $9.6 \times 10^{-14}$

g-band uncertainty =  $7.6 \times 10^{-14}$

Stellar mass estimate\* =  $6.62 \times 10^6 M_{\odot}$

Apparent r-band magnitude  $< 1 r_{\text{eff}}^* = 19.9912$

R.A. (deg)*	Decl. (deg)*	$R_{\text{eff}}^*$ (arcsec)	PA* (deg)	arat*	Alternative names*
054.2611	-34.8755	5.333780	52.031101	0.940800	FCC185, LEDA 74783, NGFS033703-34523



Pixel radius = 26

g-r		error g-r		g-band		error g-band		r-band		error r-band		Weighted $r/r_{\text{eff}}$	
UB	VB	UB	VB	UB	VB	UB	VB	UB	VB	UB	VB	UB	VB
0.614	0.614	0.022	0.022	28.204	28.205	0.020	0.020	27.589	27.591	0.009	0.009	0.121	0.121
0.621	0.616	0.023	0.023	28.276	28.274	0.021	0.021	27.655	27.658	0.009	0.009	0.288	0.288
0.613	0.615	0.031	0.032	28.598	28.614	0.029	0.029	27.984	27.998	0.013	0.013	0.556	0.555
0.637	0.630	0.060	0.064	29.303	29.375	0.055	0.059	28.666	28.745	0.024	0.026	0.926	0.922
0.644	0.624	0.105	0.108	29.919	29.938	0.097	0.098	29.275	29.314	0.042	0.044	1.298	1.300
0.640	0.703	0.146	0.172	30.269	30.460	0.133	0.159	29.629	29.758	0.058	0.066	1.674	1.664
0.717	0.742	0.438	0.480	31.477	31.579	0.406	0.446	30.760	30.838	0.165	0.178	2.267	2.326
0.677	0.761	1.221	1.032	32.584	32.413	1.125	0.961	31.907	31.652	0.475	0.376	3.326	3.347
0.507	0.884	1.842	2.231	33.000	33.265	1.651	2.106	32.493	32.381	0.816	0.735	4.108	4.174
0.684	0.987	1.543	3.332	32.839	33.710	1.423	3.175	32.155	32.724	0.597	1.009	5.229	5.074
0.615	1.056	2.761	5.760	33.460	34.311	2.521	5.520	32.844	33.255	1.128	1.645	5.787	5.938
2.083	5.749	10.995	1480.160	35.052	40.382	10.922	1480.148	32.969	34.633	1.264	5.856	6.928	6.131

## The use of Voronoi binning in obtaining Colour profiles of FDS dwarfs

### FDS10\_DWARF189

*This is the biggest and brightest (appearing) source in the sample.*

*The source was still very prominent in the cropped image, causing the large uncertainty.*

Sampled uncertainty in the background:

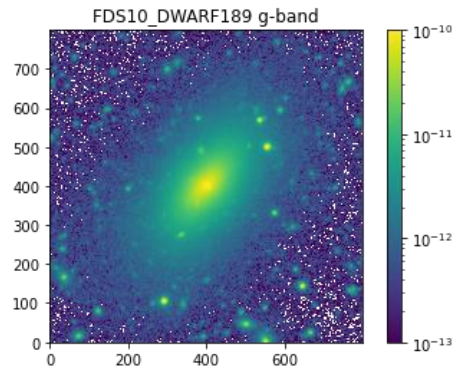
r-band uncertainty =  $2.1e-13$

g-band uncertainty =  $1.5e-13$

Stellar mass estimate\* =  $4.53e8 M_{\odot}$

Apparent r-band magnitude  $< 1 r_{\text{eff}}^* = 15.4762$

R.A. (deg)*	Decl. (deg)*	$R_{\text{eff}}^*$ (arcsec)	PA* (deg)	arat*	Alternative names*
054.5382	-34.5188	16.044941	-39.381302	0.545400	FCC203, ESO 358-42, [JPB2015] 054.5380257-34.5184045, [JPB2015] 054.5381637-34.5



Pixel radius = 80

g-r		error g-r		g-band		error g-band		r-band		error r-band		Weighted $r/r_{\text{eff}}$	
UB	VB	UB	VB	UB	VB	UB	VB	UB	VB	UB	VB	UB	VB
0.629	0.629	0.003	0.003	25.224	25.224	0.002	0.002	24.594	24.594	0.001	0.001	0.149	0.149
0.663	0.663	0.004	0.004	25.669	25.669	0.003	0.003	25.005	25.005	0.002	0.002	0.295	0.295
0.683	0.683	0.006	0.006	26.239	26.239	0.005	0.005	25.557	25.557	0.003	0.003	0.483	0.483
0.682	0.682	0.011	0.011	26.794	26.794	0.009	0.009	26.112	26.112	0.005	0.005	0.687	0.687
0.676	0.676	0.020	0.020	27.461	27.461	0.016	0.016	26.785	26.785	0.009	0.009	0.964	0.964
0.663	0.663	0.039	0.038	28.181	28.181	0.031	0.031	27.518	27.518	0.017	0.017	1.350	1.350
0.669	0.670	0.069	0.069	28.814	28.815	0.055	0.055	28.145	28.145	0.030	0.030	1.729	1.729
0.664	0.665	0.112	0.112	29.340	29.342	0.090	0.090	28.676	28.677	0.049	0.049	2.121	2.122
0.695	0.696	0.166	0.167	29.781	29.789	0.135	0.136	29.086	29.092	0.071	0.072	2.525	2.523
0.700	0.691	0.223	0.226	30.101	30.110	0.181	0.183	29.401	29.419	0.095	0.097	2.906	2.907
0.671	0.679	0.314	0.312	30.464	30.459	0.253	0.252	29.793	29.780	0.136	0.135	3.478	3.482
0.723	0.711	0.379	0.391	30.686	30.714	0.311	0.319	29.962	30.003	0.160	0.166	4.177	4.169

## The use of Voronoi binning in obtaining Colour profiles of FDS dwarfs

FDS10\_DWARF359

Sampled uncertainty in the background:

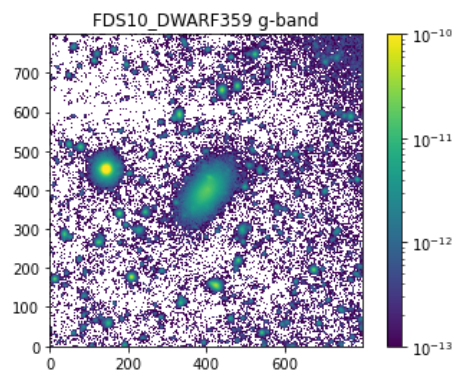
r-band uncertainty =  $9.6e-14$

g-band uncertainty =  $7.7e-14$

Stellar mass estimate\* =  $2.88e7 M_{\odot}$

Apparent r-band magnitude  $< 1 r_{\text{eff}}^* = 18.374$

R.A. (deg)*	Decl. (deg)*	$R_{\text{eff}}^*$ (arcsec)	PA* (deg)	arat*	Alternative names*
054.1791	-34.1590	8.016240	-34.378502	0.530700	FCC173, LEDA 74776



Pixel radius = 40

g-r		error g-r		g-band		error g-band		r-band		error r-band		Weighted $r/r_{\text{eff}}$	
UB	VB	UB	VB	UB	VB	UB	VB	UB	VB	UB	VB	UB	VB
0.521	0.521	0.007	0.007	26.884	26.884	0.006	0.006	26.363	26.363	0.003	0.003	0.066	0.066
0.539	0.539	0.007	0.007	26.951	26.951	0.006	0.006	26.412	26.412	0.003	0.003	0.146	0.146
0.561	0.561	0.008	0.008	27.143	27.143	0.008	0.008	26.582	26.582	0.004	0.004	0.295	0.295
0.572	0.572	0.011	0.011	27.404	27.405	0.010	0.010	26.832	26.833	0.005	0.005	0.485	0.485
0.591	0.591	0.014	0.014	27.739	27.740	0.013	0.013	27.148	27.149	0.006	0.006	0.665	0.665
0.615	0.620	0.021	0.021	28.172	28.178	0.019	0.019	27.557	27.558	0.009	0.009	0.860	0.860
0.635	0.631	0.047	0.054	29.028	29.189	0.043	0.049	28.393	28.558	0.019	0.022	1.218	1.174
0.655	0.691	0.133	0.202	30.166	30.625	0.122	0.186	29.512	29.934	0.054	0.079	1.696	1.618
0.649	0.698	0.318	0.333	31.113	31.171	0.291	0.307	30.465	30.473	0.129	0.130	2.115	2.115
0.705	0.731	1.008	0.744	32.374	32.048	0.929	0.689	31.668	31.317	0.391	0.283	2.527	2.745
0.618	0.821	1.674	1.297	32.910	32.663	1.523	1.213	32.292	31.842	0.694	0.459	2.910	3.359
6.611	1.014	1255.848	2.151	40.200	33.233	1255.846	2.051	33.589	32.219	2.294	0.649	3.251	3.899
-	1.361	14.181	4.188	-	33.980	13.996	4.081	33.583	32.619	2.281	0.939	4.108	4.336
-	2.494	20.831	17.241	-	35.541	20.732	17.185	33.451	33.047	2.019	1.392	3.887	4.916
-	3.189	5.790	31.917	-	36.212	5.219	31.888	33.686	33.023	2.508	1.362	6.172	5.874

## Appendix D: Image series 0-5

This appendix details the journey that led to the final series of images, series 6, presented in chapter 6, in further detail.

Series 0: Astropy's `make_lupton_rgb()` (`d#_ugr.png`)

Images in this series were made using Astropy's `make_lupton_rgb`-function. The function takes in three fits files and has a 'stretch' parameter, which sets the limits. Using NGC1427A (FDS11\_DWARF519) to calibrate, the stretch was chosen to be  $1.9433 \times 10^{-10}$ . Next rgu- and rgi-images were computed. The images came out very dark and in hues of orange and purple for rgu- and rgi- respectively. As in many images the dwarf galaxy itself was not visible, it was chosen to compute the images using different programs, i.e. ds9 or aladin, in future series. Depicted below is the rgu-image of FDS11\_DWARF047, which can be compared to its series 1 equivalent.

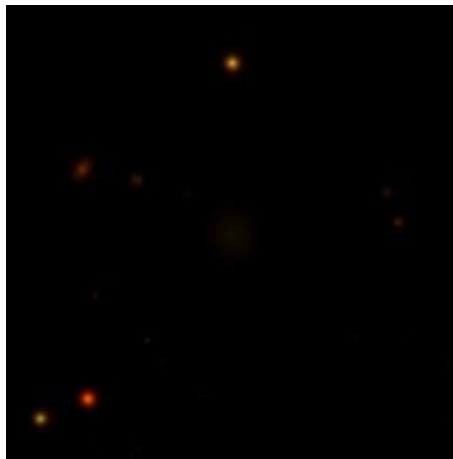


Figure D.1: `d47_ugr.png`

Series 1: ASINH DS9 (`ds9_d#_ugr.png`)

The first round of `rgb` images was made from the original (non-logarithmic) fits-files using ds9. The settings in ds9 were the same for all dwarf galaxies. For the rgu-images, an ASINH-scale function (the inverse hyperbolic sine) was chosen and limits were set to  $[-1.7281e-12; +6.4852e-11]$ . These settings were calibrated to FDS11\_DWARF069 and the limits were determined by examining the pixel distribution.

The irg-images also use an ASINH-scale function but were calibrated to FDS11\_DWARF010. The limits in these images are  $[-4.35477e-12; +2.00000e-10]$ .

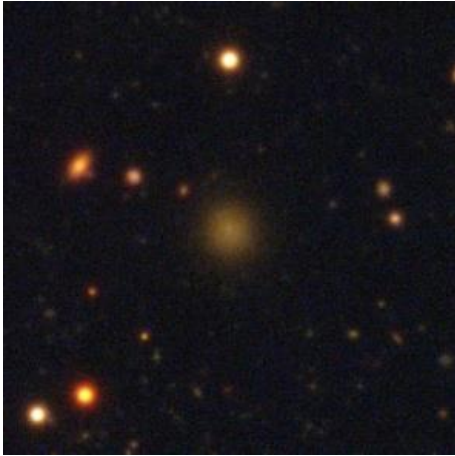


Figure D.2: ds9\_d47\_ugr.png

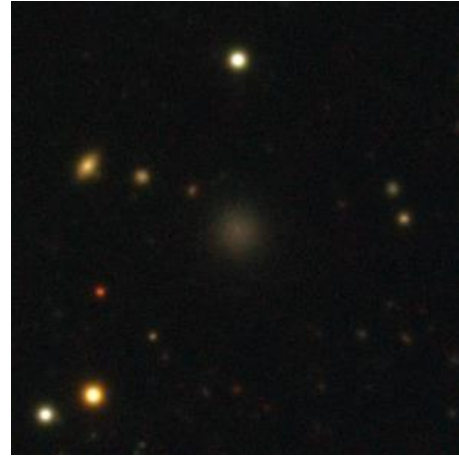


Figure D.3: ds9\_d47\_gri.png

As illustrated by the images of FDS11\_DWARF047 above, the images in this series are not bright, especially in the *igr*-series hardly any details are visible. The images do have colours that could be seen as realistic and the background appears black, as is desired.

#### Series 2: LOG DS9 (ds9\_d#\_ugr\_log.png)

This series was made using the logarithmic fits files. The scale function for images in this series is SQUARED and the boundary magnitudes are 20 and 30. As the value of most pixels lies within this range, the source does not appear in full detail. After this series of images, histograms of the data were made. From the histograms it became apparent that most of the fits files, especially those in the *i*- and *u*-band needed to be scaled.

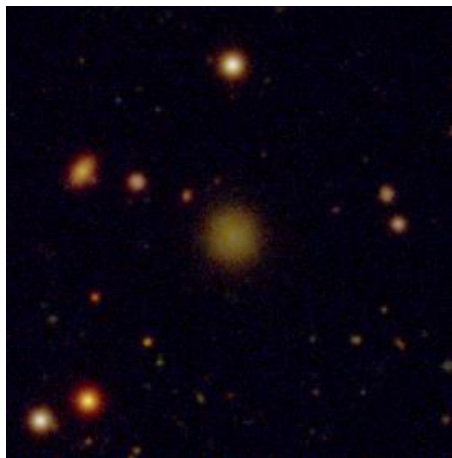


Figure D.4: ds9\_d47\_ugr\_log.png

#### Automation

In all the previous series, except for series 0, the settings were adjusted manually per image. As this is inefficient when one wants to make *rgb*-images of many dwarf galaxies, it was investigated how to automatize the creation of *rgb* images. The following series were computed by running *ds9* via a python environment and iterating over the list of tile 11 dwarf galaxies.

#### Series 3: logarithmic images (autod#/ds9\_ugr.png)

This series uses the SQUARED-scale function and has a range from 26.24 to 29.99 magnitudes. This range was chosen as most values are fainter than 26.24 yet the value 30 background is excluded. The SQUARED -scale function was chosen because it provided the best looking image during calibration.



## The use of Voronoi binning in obtaining Colour profiles of FDS dwarfs

The calibration was done using the faintest tile 11 dwarf galaxies as example and thus even faint sources appear clearly on these images. The downside of these settings are that the centres of bright galaxies, like FDS11\_DWARF339, appear overexposed.

Series 4: bright logarithmic images (autod#/ds9\_ugr\_bright.png)

Using NGC1427A for calibration, it became apparent that by changing the scale function to LINEAR, the centre of bright sources did show details. This resulted in this second regime of image settings.

Series 5: bright linear images (autod#/ds9\_ugr\_bright\_lin.png)

This series uses the regular fits files instead of the logarithmic ones. The limits are [1e-12:1e-9] and the scale function is LOG.

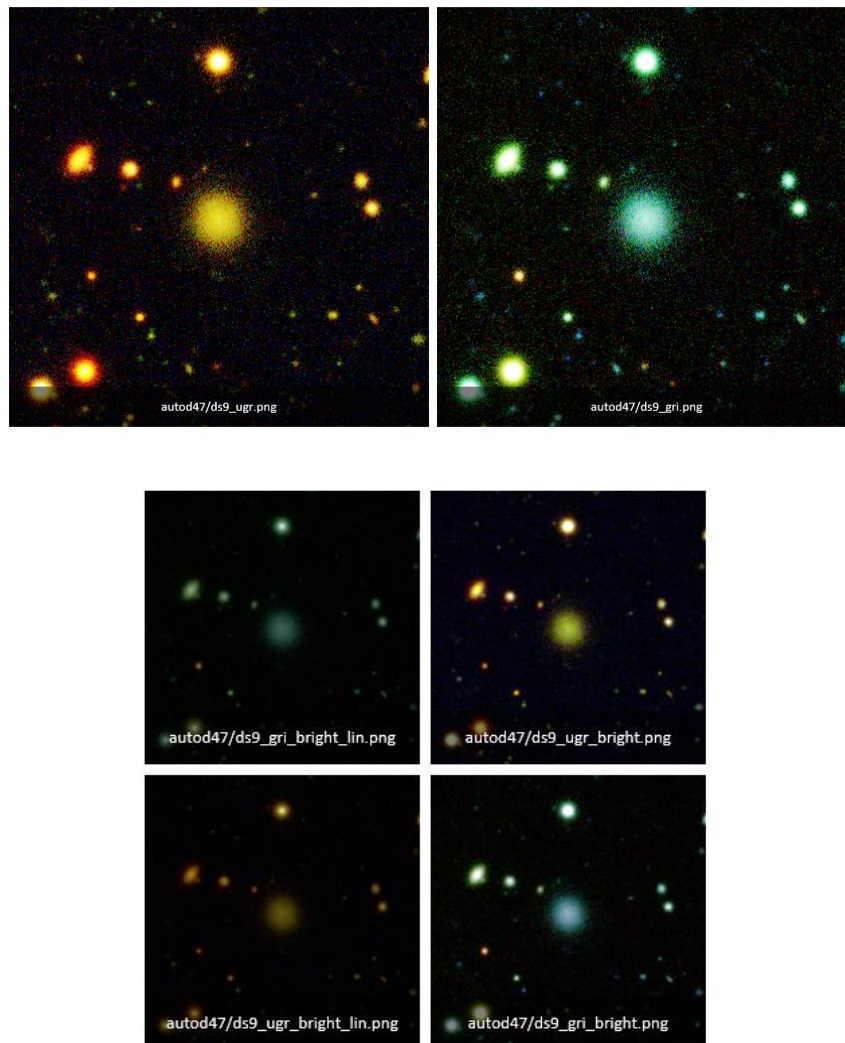


Figure D.5: FDS11\_DWARF047



## Appendix E: scripts

Python scripts are provided in the following order:

1. Cropping a large data set into smaller ones based on a table with coordinates, including linear background correction function
2. Histogram based background correction function
3. List making function (input VorBin)
4. Function for applying the VorBin output
5. Spherical and Elliptical profile function

In [2]:

```
import numpy as np
import matplotlib.pyplot as plt
from astropy.io import fits
import random
from matplotlib.colors import LogNorm
from scipy.stats import mode
%matplotlib inline

def cor2pixt11(ra,dec, rad, header):
    """Converts a R.A. and Dec. in degrees and radius in arcseconds to pixels for tile 11"""
    xpc = 12305.0
    ypc = -8389.0
    xc = 54.5
    yc = -35.5

    xstep = -(5.555555638E-05)/np.cos(np.deg2rad(dec)) #spherical coordinates require a cos
    ystep = 5.555555638E-05

    xc0 = xc - xpc*xstep
    yc0 = yc - ypc*ystep

    px = int((ra-xc0)/xstep)
    py = int((dec-yc0)/ystep)

    radius = int((rad/3600)/ystep)

    header['CRVAL1'] = ra #Correcting the header.
    header['CRVAL2'] = dec
    header['CRPIX1'] = px
    header['CRPIX2'] = py

    return px, py, radius, header

def plotit(picture):
    """Plots a fits image using logscale and regular axes."""
    #mapp = colourmania()
    mapp = 'inferno'
    plt.imshow(picture, cmap=mapp, norm=LogNorm())
    plt.gca().invert_yaxis()
    plt.colorbar()
    plt.show()

def save(name,letter,file, header):
    """Saves a file as fits file under a specified name."""
    outfile = 'Your location here/'+name+'/'+name + letter + '+' + '.fits'
    hdu = fits.PrimaryHDU(file,header)
    hdu.writeto(outfile,overwrite=True)

def savelog(name,letter,file, header):
    """Saves a file as fits file under a specified name."""
    outfile = 'Your location here/'+name+'/'+name + letter + 'maglog'+ '.fits'
    hdu = fits.PrimaryHDU(file,header)
    hdu.writeto(outfile,overwrite=True)

def backgroundreduce(data,r,name,band):
    """Reduces background noise via addition of a linear value
    if the median of the background is larger than the standard deviation."""

    #create the length of small squares.
```

```

if data.shape[0] > 100:
    dx = int(data.shape[0]/100)
    dy = int(data.shape[1]/100)
else:
    dx = 9
    dy = 9

#create the starting square and path in y.
X = 0
Y = np.arange(0,data.shape[1],dy)

#set the forbidden area.-> succes depends on the accuracy of the table data...
pxcenterx = int(data.shape[0]/2)
pxcentery = int(data.shape[0]/2)

pxrx = 8*r
pxry = 8*r

#create some squares and compute their median
M = []

while X < pxcenterx - pxrx:
    for y in Y:
        M.append(np.median(data[X:X+dx,y:y+dy]))
    X = X + dx
while X < pxcenterx + pxrx:
    X = X + dx
while X < data.shape[0]-dx:
    for y in Y:
        M.append(np.median(data[X:X+dx,y:y+dy]))
    X = X + dx

#Compute the median and standarddeviation.
m = np.median(M)
std = np.std(M)

#Determine wether the background needs adjustment or not.
if abs(m) > std/10:
    newdata = data - m
else:
    newdata = data #Optional, gives indication of whether the corrections happen often
    print('No correction needed.')
    print('name and band: ',name, band)
    print('median: ', m)
return newdata

def makelog(data):
    """Creates the log version fo an image."""
    m = np.median(data)
    for i in range(0,int(data.shape[0])):
        for j in range(0,int(data.shape[1])):
            if data[i,j] <= 0:
                data[i,j] = abs(m/10) #we set it to a small yet positive value...
    return -2.5*np.log10(data)

def plotlimit(data):
    "Sets the maximum magnitude to 30."
    for i in range(0,int(data.shape[0])):
        for j in range(0,int(data.shape[1])):
            if data[i,j] > 30:

```

```
return data      data[i,j] = 30 #we set it to a small yet positive value...
```

In [59]:

```
#Function that uses the fucntions from the cell above...

def cropalot(data, letter, file,header):
    """crops all areas from a specified table and saves them under a numberbased name."""
    nr = file[:,0]
    RA = file[:,1]
    Dec = file[:,2]
    Rad = file[:,3]

    #Here we save the dwarf names
    Name = []
    for i in range(0,len(nr)):
        name = 'd' + str(int(nr[i]))
        Name.append(name)

    #Next we convert the coordinates and radius to pixels.
    X = []
    Y = []
    R = []
    H = []

    for i in range(0,len(nr)):
        x,y,rn, h = cor2pixt11(RA[i],Dec[i],Rad[i], header)
        H.append(h)
        X.append(x)
        Y.append(y)
        R.append(10*rn) #The sample dwarfs appeared well on the slices with this value.

    #Now we crop the data from the original tile.
    CROP = []

    for i in range(0,len(nr)):
        crop = data[np.int(Y[i]-R[i]):np.int(Y[i]+R[i]),np.int(X[i]-R[i]):np.int(X[i]+R[i])]
        CROP.append(crop)

    #Here we adjust the background if needed.
    for i in range(0,len(nr)):
        new = backgroundreduce(CROP[i],int(R[i]/10),Name[i],letter)
        CROP[i] = new

    #Now we save the images
    for i in range(0,len(nr)):
        save(Name[i],letter,CROP[i],H[i])
        plotit(CROP[i]) #Optional, set it to plot instead when just testing.
        print('Figure: ',Name[i],letter)

    #Finally let's save the Log version
    for i in range(0,len(nr)):
        logfile = makelog(CROP[i])
        name = Name[i]
        # name = 'magLog' + Name[i]

        logfile2 = plotlimit(logfile)

        mapp = 'inferno_r'
        plt.imshow(logfile2, cmap=mapp) #Optional, set it to plot instead when just testing
        plt.gca().invert_yaxis()
        plt.colorbar()
```

```
plt.title(name)
plt.show()
```

```
savelog(name,letter,logfile2,H[i])
```

```
def multibandslice(mapp,filename,file):
    """This formula crops a list of dwarf galaxies,
       specified in the cropalot function
       from a tile in all four bands."""

    letters = ['i','r','g','u'] #'r','g',

    for i in range(0,len(letters)):
        name = mapp+letters[i]+ filename
        image = fits.open(name)
        header = image[0].header
        data = image[0].data
        cropalot(data,letters[i],file,header)
```

```

In [ ]: from astropy.io import fits
import matplotlib.pyplot as plt
import numpy as np
%matplotlib inline

def colourplot(name):
    """This function makes 4-band pixeldistributionplots"""

    letters = ['i', 'r', 'g', 'u']
    Flat = [] #The flattend data without the 30magnitude boundary

    for i in range(0, len(letters)):
        nam = 'Your locaiton here/' + name + '/' + name + letters[i] + '.fits'
        image = fits.open(nam)
        data = image[0].data
        flatn = data.flatten()
        flattend = [i for i in flatn if i != 30]
        Flat.append(flattend)
    saveloc = 'Your location here/' + name + '/' + name + 'pixelplotscaled.png'

    plt.title(name)
    plt.xlabel("value")
    plt.ylabel("pixels Frequency")
    plt.hist(Flat[2], range=[-1e-11, 1e-11], bins=200, log=True, histtype='step', color='chartreuse', label='g-band')
    plt.hist(Flat[1], range=[-1e-11, 1e-11], bins=200, log=True, histtype='step', color='orangered', label='r-band')
    plt.hist(Flat[0], range=[-1e-11, 1e-11], bins=200, log=True, histtype='step', color='maroon', label='i-band')
    plt.hist(Flat[3], range=[-1e-11, 1e-11], bins=200, log=True, histtype='step', color='slateblue', label='u-band')
    plt.plot()
    plt.legend(loc='upper right')
    plt.savefig(saveloc, rename=True)
    plt.show()

def makelog(data):
    """Creates the log version of an image."""
    m = np.median(data)
    for i in range(0, int(data.shape[0])):
        for j in range(0, int(data.shape[1])):
            if data[i, j] < 1e-12:
                data[i, j] = 1e-12 #we set it to a small yet positive value...
    return -2.5*np.log10(data)

def save(name, letter, file, header):
    """Saves a file as fits file under a specified name."""
    outfile = name + letter + '.fits'
    hdu = fits.PrimaryHDU(file, header)
    hdu.writeto(outfile)

def openandscale(name, letter, value, magval):
    """correctes a fits via multiplication with a specified value."""
    nam = 'Your location here/' + name + '/' + name + letter + '.fits'
    image = fits.open(nam)
    header = image[0].header
    data = image[0].data
    if magval == True:
        val = 10**(value/(-2.5))
    else:
        val = value
    data *= val

    nam2 = 'Your location here/' + name + '/n' + name + letter + '.fits'
    nam3 = 'Your location here/' + name + '/nmaglog' + name + letter + '.fits'

    hdu = fits.PrimaryHDU(data, header)
    hdu.writeto(nam2, overwrite=True)

    logdat = makelog(data)
    hdu2 = fits.PrimaryHDU(logdat, header)
    hdu2.writeto(nam3, overwrite=True)

```



In [6]:

```
import numpy as np

def maketable(data,name,mask,letter):
    """Makes a table from a fits file whilst applying a mask"""
    path = 'Your location here/'+ name + '/' + name + letter + '.txt' #target location
    table = open(path,'w')
    table.write("X Y S N \n")
    noise = np.std(data/100) #noise
    for i in range(0,int(data.shape[0])):
        for j in range(0,int(data.shape[1])):
            if mask[i,j] == 0:
                line = str(i)+" "+str(j)+" "+str(data[i,j]- 9e-13)+" "+str(noise)+" \n"
                table.write(line)

    table.close()
```

In [2]:

```
import numpy as np
from astropy.io import fits

StN = [100] #The target signal to noise in the Voronoi binning.
for i in range(0,len(StN)):
    """Applies the Voronoi bins to a dataset in the g- and r-band"""
    name='d'+str(int('galaxy number here'))
    image = fits.open('Your location here'+ name + '/' + name + 'g.fits')
    imager = fits.open('Your location here'+ name + '/' + name + 'r.fits')

    listloc = 'Your location here'+ 'DATA_' + name + 'r' + '.txt' #output of VorBin
    bins = np.loadtxt(listloc)
    file = 'Your location here'+name+ '/' + name + 'r' + '.txt' #output of table making f
    datal = np.loadtxt(file,usecols=0,skiprows=1)
    Xval = datal #vertical
    datay = np.loadtxt(file,usecols=1,skiprows=1)
    Yval = datay #horizontal
    mask = fits.open('Mask file')[0].data

    savelog= 'Your location here'+ 'voronoi' + name + str(int(StN[i])) + 'g' + '.fits'
    savelogr= 'Your location here'+ 'voronoi' + name + str(int(StN[i])) + 'r' + '.fits'

    data = image[0].data
    datar = imager[0].data
    header = image[0].header
    uni = np.unique(bins) #amount of unique bins

    for u in range(0,len(uni)):
        count = [] #All pixels belonging to this bin
        values = [] #The value of said pixels (will be set to median...)
        valuesr = []
        for i in range(0,len(bins)): #finds values and adresses
            if int(uni[u]) == int(bins[i]):
                count.append(i)
                if mask[np.int(Xval[i]),np.int(Yval[i])] == 0: #only taking the masked value
                    values.append(data[np.int(Xval[i]),np.int(Yval[i])])
                    valuesr.append(datar[np.int(Xval[i]),np.int(Yval[i])])
        newvalue = np.median(values) #calculates the new value
        newvaluer = np.median(valuesr)

        for j in range(0,len(count)): #replaces the old value
            data[np.int(Xval[count[j]]),np.int(Yval[count[j]])] = newvalue
            datar[np.int(Xval[count[j]]),np.int(Yval[count[j]])] = newvaluer

    hdu1 = fits.PrimaryHDU(data,header)
    hdu1.writeto(savelog,overwrite=True)

    hdu2 = fits.PrimaryHDU(datar,header)
    hdu2.writeto(savelogr,overwrite=True)
```

```

In [ ]: import numpy as np
import matplotlib.pyplot as plt
from astropy.io import fits
from matplotlib.colors import LogNorm
import pandas as pd
%matplotlib inline

def rad2pix(rad):
    """converts the radius from arcseconds to pixels."""
    ystep = 5.55555638E-05
    radius = int((rad/3600)/ystep)
    print('The pixel radius is: ',radius)
    return radius

def ringvalue2(datar,datag,dist,mask,reff,datai,datou):
    """Selects g and r in rings with distance dist[i-1]-dist[i] from the center.
    Returns lists of the values and the outer distance expressed in reff."""
    ylen,xlen = datar.shape
    center = [ylen/2,xlen/2] #get the central coordinates
    Gval = []
    Rval = []
    Uval = []
    Ival = []
    N = []
    X = []
    Y = []
    RAD = []
    Samplesize = []
    for i in range(0,len(dist)-1): #Loop till we have all rings
        R = []
        G = []
        U = []
        I = []
        Radius = 0
        Rsum = 0
        y = center[0] - dist[i] #make a ring shaped area
        while y <= center[0]+dist[i]: #stay within the ring
            for j in range(-dist[i],dist[i]): #evaluate all x,y values in the grid
                if dist[i-1] <= ((y-center[0])**2+(j)**2)**0.5 <= dist[i]: #radius condition
                    if mask[int(y),int(center[1]+j)] == 0: #avoid usig masked values
                        R.append(datar[int(y),int(center[1]+j)])
                        G.append(datag[int(y),int(center[1]+j)])
                        U.append(datou[int(y),int(center[1]+j)])
                        I.append(datai[int(y),int(center[1]+j)])
                        Y.append(int(y))
                        X.append(int(center[1]+j))
                        Radius += ((y-center[0])**2+(j)**2)**0.5*datar[int(y),int(center[1]+j)]
                        Rsum += datar[int(y),int(center[1]+j)]
                    y+=1
            Samplesize.append(len(R)) #To get an indication how many pixels are used per ring.
            N.append(dist[i]/reff)
            if Rsum != 0:
                RAD.append(Radius/Rsum)
            Rmean = np.mean(R)
            Gmean = np.mean(G)
            Gval.append(Gmean)
            Rval.append(Rmean)
            Umean = np.mean(U)
            Imean = np.mean(I)
            Uval.append(Umean)
            Ival.append(Imean)

    return Gval, Rval, N, Samplesize, X, Y, Ival, Uval,RAD

def ellipse(datar,datag,dist,mask,xx,yy,arat,theta,reff):
    """Selects g and r in elliptical rings with distance dist[i-1]-dist[i] from the center.
    Returns lists of the values and the outer distance expressed in reff."""
    Gval = []
    Rval = []
    N = []
    X = []
    Y = []
    RAD = []
    Samplesize = []
    for i in range(1,len(dist)): #Loop till we have all rings
        R = []
        G = []
        Radius = 0
        rrr = 0
        for x in range(-dist[i],dist[i]):
            for y in range(-dist[i],dist[i]):
                value = (x*np.cos(theta)-y*np.sin(theta))**2/dist[i]**2+(x*np.sin(theta)+y*np.cos(theta))**2/(arat*dist[i])**2
                oldvalue = (x*np.cos(theta)-y*np.sin(theta))**2/dist[i-1]**2+(x*np.sin(theta)+y*np.cos(theta))**2/(arat*dist[i-1])**2
                if value <= 1 < oldvalue: #radius condition
                    if mask[int(y+yy),int(x+xx)] == 0: #avoid usig masked values
                        R.append(datar[int(y+yy),int(x+xx)])
                        G.append(datag[int(y+yy),int(x+xx)])
                        Y.append(int(y+yy))
                        X.append(int(x+xx))
                        Radius += np.sqrt((y**2+x**2))*datar[int(y+yy),int(x+xx)]
                        rrr += datar[int(y+yy),int(x+xx)]
            Samplesize.append(len(R)) #To get an indication how many pixels are used per ring.
            N.append(dist[i]/reff)
            Rmean = np.mean(R)
            Gmean = np.mean(G)
            Gval.append(Gmean)
            Rval.append(Rmean)
            RAD.append(Radius/rrr)

    return Gval, Rval, N, Samplesize, X, Y,RAD

```

## Error Propagation

The errors shown in the colour diagrams presented in this report are computed in the following way:

First, the mean of the background is sampled in several handpicked boxes which do not appear to contain any (bright) sources. The standard deviation of the mean in all these boxes is computed and the resulting constant is considered the systematic error in the dataset. Next, the relative error is computed for each individual pixel.

As shown in chapter 4, the colour (here  $g-r$ , but it works similarly for other bands) is computed using:

$$g - r = 2.5 \log_{10} \left( \frac{F_r}{F_g} \right)$$

Given the relative error in two bands,  $r$  and  $g$ , the error in  $g-r$  is:

$$\begin{aligned} \text{Let } Q = \frac{F_r}{F_g}, \text{ then } \frac{\Delta Q}{Q} &= \sqrt{\left(\frac{\Delta F_r}{F_r}\right)^2 + \left(\frac{\Delta F_g}{F_g}\right)^2} \\ \text{Let } Z = 2.5 \log_{10} Q, \text{ then } \Delta Z &= |f'(Q)| \Delta Q \\ &= 1.08574 \frac{\Delta Q}{Q} = 1.08574 \sqrt{\left(\frac{\Delta F_r}{F_r}\right)^2 + \left(\frac{\Delta F_g}{F_g}\right)^2} \end{aligned}$$

The error in  $g-r$  is thus given by:

$$\Delta_{g-r} = 1.08574 \sqrt{\left(\frac{\Delta F_r}{F_r}\right)^2 + \left(\frac{\Delta F_g}{F_g}\right)^2}$$